

**The E3 ubiquitin ligase TRIM23 regulates adipocyte differentiation via
stabilization of the adipogenic activator PPAR γ**

**Masashi Watanabe¹, Hidehisa Takahashi¹, Yasushi Saeki², Takashi Ozaki¹, Shihori
Itoh¹, Masanobu Suzuki¹, Wataru Mizushima¹, Keiji Tanaka², Shigetsugu
Hatakeyama^{1,*}**

¹Department of Biochemistry, Hokkaido University Graduate School of Medicine, Kita
15, Nishi 7, Kita-ku, Sapporo, Hokkaido 060-8638, Japan.

²Laboratory of Protein Metabolism, Tokyo Metropolitan Institute of Medical Science,
Setagaya-ku, Tokyo 156-8506, Japan

*Corresponding author: Shigetsugu Hatakeyama, MD., Ph.D. Department of
Biochemistry, Hokkaido University Graduate School of Medicine, Kita 15, Nishi 7,
Kita-ku, Sapporo, Hokkaido 060-8638, Japan. E-mail: hataas@med.hokudai.ac.jp,
Phone: +81-11-706-5899, Fax: +81-11-706-5169

Competing interests: The authors declare that no competing interests exist.

20 **Abstract**

21

22 Adipocyte differentiation is a strictly controlled process regulated by a series of
23 transcriptional activators. Adipogenic signals activate early adipogenic activators and
24 facilitate the transient formation of early enhanceosomes at target genes. These
25 enhancer regions are subsequently inherited by late enhanceosomes. PPAR γ is one of
26 the late adipogenic activators and is known as a master regulator of adipogenesis.
27 However, the factors that regulate PPAR γ expression remain to be elucidated. Here, we
28 show that a novel ubiquitin E3 ligase, tripartite motif protein 23 (TRIM23), stabilizes
29 PPAR γ protein and mediates atypical polyubiquitin conjugation. TRIM23 knockdown
30 caused a marked decrease in PPAR γ protein abundance during preadipocyte
31 differentiation, resulting in a severe defect in late adipogenic differentiation, whereas it
32 did not affect the formation of early enhanceosomes. Our results suggest that TRIM23
33 plays a critical role in the switching from early to late adipogenic enhanceosomes by
34 stabilizing PPAR γ protein possibly via atypical polyubiquitin conjugation.

35

36 **Introduction**

37

38 Adipose tissue is a major storehouse for excess energy and has recently been shown to
39 be an endocrine tissue critical for the generation of hormones and cytokines involved in
40 energy metabolism (*Galic et al., 2010*). Abnormalities in adipocyte differentiation or
41 functions may result in the development of metabolic syndrome by inducing insulin
42 resistance, and these abnormalities are likely to be induced in part by inappropriate
43 regulation of gene expression required for adipocyte differentiation or functions.

44 The conversion of preadipocytes to mature adipocytes is a strictly controlled process
45 regulated by a series of transcriptional activators. Both *in vivo* and *in vitro* studies have
46 shown that peroxisome proliferator-activated receptor γ (PPAR γ) and three
47 CCAAT/enhancer family members (α , β , and δ) are essential regulators of adipogenesis
48 (*Barak et al., 1999; Imai et al., 2004; Sugii et al., 2009; Tontonoz et al., 1994b; Yeh et*
49 *al., 1995*). The adipogenic program is generally composed of two steps. The first step is
50 initiated by adipogenic stimuli that induce early adipogenic activators including
51 C/EBP β , C/EBP δ and Krüppel-like factors (KLFs) and lead to the formation of early
52 enhanceosomes (*Mori et al., 2005; Oishi et al., 2005*). In the second step, these early
53 enhanceosomes induce late adipogenic activators including PPAR γ and C/EBP α that
54 lead to terminal differentiation by inducing genes necessary for the characteristics of
55 mature adipocytes (*Lefterova et al., 2008; Rosen et al., 2002*).

56 Recent studies using high-throughput sequencing have shown that transcriptional
57 activators do not function individually but rather cooperate with other activators and

58 form hotspots at specific genomic regions (*Boergesen et al., 2012; Chen et al., 2008;*
59 *Gerstein et al., 2012; He et al., 2011; Moorman et al., 2006; Siersbaek et al., 2011*). In
60 addition, the existence of super-enhancers has been recently reported (*Loven et al.,*
61 *2013; Whyte et al., 2013*). Super-enhancers are large genomic domains occupied by
62 master transcriptional activators and mediators, which induce expression of genes that
63 define cell identity, and are especially characterized by a large amount of localization of
64 Mediator subunit 1 (MED1). During the early phase of adipogenic differentiation,
65 hotspots are central constituents in super-enhancers and have been suggested to
66 cooperate with super-enhancers to drive the differentiation process (*Siersbaek et al.,*
67 *2014*). A previous study showed that C/EBP β , C/EBP δ , CREB1 and PPAR γ function as
68 candidate master transcriptional activators in adipose tissue (*Hnisz et al., 2013*). Of
69 those master transcriptional activators, PPAR γ plays a central role in adipogenesis,
70 whereas other factors cannot induce adipocyte differentiation in the absence of PPAR γ
71 (*Farmer, 2006; Rosen and MacDougald, 2006*).

72 PPAR γ has two isoforms, PPAR γ 1 and PPAR γ 2. These two isoforms are generated
73 from alternate promoter usage and splicing, and PPAR γ 2 contains 30 additional amino
74 acids at the amino-terminus (*Fajas et al., 1997; Tontonoz and Spiegelman, 2008; Zhu et*
75 *al., 1995*). PPAR γ 1 is ubiquitously expressed and PPAR γ 2 is strictly expressed in
76 adipose tissues, while both isoforms are strongly induced during adipocyte
77 differentiation. Although ectopic expression of either of the PPAR γ isoforms can induce
78 adipocyte differentiation, PPAR γ 2 is thought to play a more central role in this process
79 (*Mueller et al., 2002; Zhang et al., 2004*). It has been reported that PPAR γ expression

80 and activity are regulated at different levels such as transcription, protein degradation
81 and post-translational modification levels (*Ahmadian et al., 2013; Eeckhoutte et al.,*
82 *2012; Lee and Ge, 2014; van Beekum et al., 2009*).

83 Tripartite motif-containing (TRIM) proteins (also known as E3 ubiquitin–protein
84 ligases) are characterized by the presence of a RING finger, one or two zinc-binding
85 motifs called B-boxes, and an associated coiled-coil region (RBCC), and there are
86 currently known to be 77 TRIM proteins in humans. TRIM family proteins are involved
87 in a broad range of biological processes, and their alterations result in diverse
88 pathological conditions (*Hatakeyama, 2011; Meroni and Diez-Roux, 2005; Ozato et al.,*
89 *2008*). TRIM23 is a member of the TRIM family and possesses carboxy-terminal ARF
90 (ADP ribosylation factor) domains. A recent study has shown that TRIM23 mediates
91 atypical lysine 27 (K27)-linked polyubiquitin conjugation to NEMO, which plays an
92 important role in the NFκB pathway, and this conjugation is essential for TLR3- and
93 RIG-I/MDA5-mediated antiviral innate and inflammatory responses (*Arimoto et al.,*
94 *2010*).

95 In this study, we identified TRIM23 as a novel factor that regulates PPARγ protein
96 stability, possibly via atypical ubiquitin conjugation to PPARγ. TRIM23 knockdown
97 caused reduction of PPARγ protein levels, which were restored by treatment with a
98 proteasome inhibitor, leading to a severe defect in adipogenic differentiation. TRIM23
99 is dispensable for the early adipogenic program but is indispensable for the late
100 adipogenic program. By controlling PPARγ abundance, TRIM23 functions as a
101 regulator for a critical link between early and late enhanceosomes.

103 **Results**

104

105 **TRIM23 is expressed in mouse adipose tissue during adipogenesis**

106 To determine whether TRIM23 is involved in adipocyte differentiation, we first
107 examined the expression of TRIM23 during differentiation of 3T3-L1 cells and in
108 mouse adipose tissue. Real-time PCR analysis and immunoblot analysis revealed that
109 TRIM23 was expressed in preadipocytes and that mRNA and protein levels slightly
110 increased during adipogenesis (Figure 1A, B). Consistent with these results, TRIM23
111 was found to be predominantly expressed in the preadipocyte-containing stromal
112 vascular fraction (SVF) at a level as high as that in the mature adipocyte fraction
113 (Figure 1C). We also measured *Trim23* expression in a model of diet-induced obesity,
114 and we found no significant difference between the expression levels in mice receiving
115 the high-fat diet and those receiving the control chow (Figure 1C). We next examined
116 the subcellular localization of TRIM23. We fractionated 3T3-L1 cells into nuclear
117 extracts and cytoplasmic S100 fraction, and we found that a large amount of TRIM23
118 was distributed in the cytoplasm (Figure 1D).

119

120 **TRIM23 is required for adipogenesis**

121 We next examined whether TRIM23 expression was necessary for adipocyte
122 differentiation. Two different shRNAs (shTRIM23a and shTRIM23b) and a
123 non-targeting control shRNA (shControl) were introduced into 3T3-L1 preadipocytes
124 using retroviral vectors. One shRNA (shTRIM23a) efficiently depleted and the other

125 (shTRIM23b) weakly depleted TRIM23 expression levels in 3T3-L1 preadipocytes
126 relative to shControl (Figure 2A). These cells were stimulated to differentiate, and the
127 ability to undergo differentiation to mature adipocytes was evaluated by determination
128 of lipid accumulation using Oil Red O staining, direct measurement of intracellular
129 triglyceride contents and determination of relative mRNA levels of adipocyte-specific
130 genes including *Fabp4*, *Cidec*, *Klf15*, *Adipoq*, and *Retn*. Remarkably, TRIM23
131 knockdown significantly decreased lipid accumulation and markedly impaired the
132 induction of adipocyte-specific genes (Figure 2B-D and Figure 2-figure supplement 1).
133 To test whether this regulatory network is relevant to human adipocytes, we introduced
134 siRNA into human primary visceral preadipocytes and differentiated them to mature
135 adipocytes. Consistent with the results for mouse 3T3-L1 cells, TRIM23 knockdown
136 significantly decreased lipid accumulation (Figure 2B and Figure 2-figure supplement
137 2). These findings indicate that TRIM23 is required for efficient conversion of
138 preadipocytes to mature adipocytes. It has been shown that most adipocyte-specific
139 genes are PPAR γ target genes (*Lefterova et al., 2008; Nielsen et al., 2008*). We next
140 examined the occupancy of PPAR γ at a well-described PPAR γ target gene, *Fabp4*,
141 during adipocyte differentiation. PPAR γ forms heterodimers with RXR α , which
142 specifically bind to PPAR response elements (PPREs). It has been reported that PPAR γ
143 is recruited to two PPREs located 5,500 bp upstream from the transcriptional start site
144 (TSS) of the *Fabp4* gene, and this recruitment mediates activation of the *Fabp4* gene
145 (Figure 2E) (*Nielsen et al., 2006; Tontonoz et al., 1994a*). We found that TRIM23
146 depletion decreased the occupancy of PPAR γ on the enhancer PPRE at day 4 using

147 chromatin immunoprecipitation (ChIP)-qPCR analysis (Figure 2F). It has been shown
148 that some subunits of Mediator complex are necessary for the adipogenic process.
149 MED14 is required for full activation of PPAR γ -mediated transcription and adipocyte
150 differentiation *in vitro*, and MED23 is required for the early transcriptional events
151 during adipogenesis (Grontved *et al.*, 2010; Wang *et al.*, 2009). MED1 is also required
152 for adipogenesis *in vitro* (Ge *et al.*, 2002). We tested the occupancy of MED1, one of
153 the Mediator subunits, and found that TRIM23 depletion reduced the occupancy of
154 MED1 at the *Fabp4* gene at day 4 (Figure 2G). We also found reduced occupancy of Pol
155 II at the *Fabp4* gene in TRIM23 knockdown cells (Figure 2H). These findings suggest
156 that the adipogenic defect by TRIM23 knockdown is caused by reduced PPAR γ
157 recruitment and subsequent reduced transcriptional activation on the target genes.

158

159 **TRIM23 is required for induction of late adipogenic activators but not for**
160 **induction of early adipogenic activators during adipogenesis**

161 We showed that TRIM23 knockdown reduces PPAR γ recruitment to the enhancer and
162 subsequent Pol II recruitment to the promoter at the target genes. To elucidate
163 mechanisms of decreased PPAR γ -mediated gene activation in TRIM23 knockdown
164 3T3-L1 cells, we investigated mRNA levels of several adipogenic transcription factors
165 during adipogenesis. Real-time PCR analysis revealed that induction of early
166 transcriptional factors, *Cebpb* and *Cebpd*, was largely unaffected during adipocyte
167 differentiation and that the expression of late adipogenic activators, *Pparg* and *Cebpa*,
168 was equally induced at day 2 but was significantly reduced from day 4 by TRIM23

169 depletion (Figure 3). These findings suggest that an adipogenic defect by TRIM23
170 knockdown is caused by the decreased expression of late adipogenic activators.

171

172 **TRIM23 knockdown does not affect the occupancy of C/EBP β and C/EBP δ at the**
173 **PPAR γ 2 promoter during adipogenesis**

174 It has been reported that hormonal treatment of 3T3-L1 cells acutely induces the
175 expression of C/EBP β and C/EBP δ within a few hours after stimulation. These early
176 transcriptional activators have also been shown to be recruited to their target sites
177 including the *Pparg* locus (Siersbaek *et al.*, 2011; Steger *et al.*, 2010). C/EBP β marks a
178 subset of early transcription factor hotspots and forms early enhanceosomes with other
179 early adipogenic transcription factors (Siersbaek *et al.*, 2011). These early
180 enhanceosomes facilitate epigenetic modification and chromatin remodeling. To
181 determine whether TRIM23 affects PPAR γ induction, we investigated the expression
182 levels of *Cebpb* and *Cebpd* and subsequent recruitment of C/EBP β and C/EBP δ to the
183 *Pparg* locus at the early phase of adipogenesis. As shown in Figure 4A, there were little
184 differences in *Cebpb* and *Cebpd* mRNA levels between TRIM23 knockdown and
185 controls. We next examined the possibility that TRIM23 affected the occupancy of
186 C/EBP β and C/EBP δ at the *Pparg* promoter during adipogenesis using ChIP-qPCR
187 analysis (Figure 4B, C). As previously reported, C/EBP β and C/EBP δ were enriched to
188 their target sites, including *Pparg*, *Iqck*, and *Cav2* loci (Siersbaek *et al.*, 2011), but
189 TRIM23 depletion had no significant effect on this enrichment. These results suggest
190 that TRIM23 functions at the downstream stage after recruitment of early adipogenic

191 activators.

192 During differentiation, growth-arrested 3T3-L1 preadipocytes synchronously
193 re-enter the cell cycle and undergo several rounds of clonal expansion, called mitotic
194 clonal expansion (MCE) (*Tang et al., 2003b*). MCE is required for expression of
195 adipogenic proteins and progression of terminal differentiation. C/EBP β has been
196 shown to play a pivotal role in MCE (*Tang et al., 2003a*). To evaluate MCE in
197 TRIM23-knockdown cells, we counted cell numbers during adipocyte differentiation
198 (Figure 4D). However, there was no difference between TRIM23-knockdown cells and
199 the corresponding control. These findings also support the idea that TRIM23 does not
200 affect the activities of C/EBP β . Taken together, we concluded that PPAR γ 2 expression
201 by TRIM23 is not regulated through induction and occupancy of C/EBP β and C/EBP δ
202 at the *Pparg*2 promoter.

203

204 **Depletion of TRIM23 does not affect epigenetic marks and chromatin opening but**
205 **decreases the occupancy of PPAR γ itself and Pol II at the *Pparg* promoter**

206 Activators such as C/EBP β and C/EBP δ promote the recruitment of general
207 transcriptional machinery composed of general transcription factors (GTFs) and RNA
208 Pol II to form the pre-initiation complex (PIC) (*Lemon and Tjian, 2000; Thomas and*
209 *Chiang, 2006*). To achieve this goal, activators recruit GTFs and Pol II directly or
210 indirectly through binding to many cofactors. The transcription cofactors can be largely
211 classified into two groups. The first group is composed of covalent histone-modifying
212 enzymes and ATP-driven nucleosome remodelers to reorganize the chromatin

213 architecture (*Belotserkovskaya and Berger, 1999; Jaenisch and Bird, 2003; Margueron*
214 *et al., 2005*). These factors create an open chromatin environment suitable for
215 transcription. The second group consists of general cofactors such as the Mediator
216 complex and the SAGA complex (*Timmers and Tora, 2005*). The Mediator complex is
217 an evolutionarily conserved coregulatory complex that typically works in
218 communication between activators and general transcription machinery (*Malik and*
219 *Roeder, 2010*). It has been shown that some subunits of the Mediator complex are
220 necessary for the adipogenic process (*Ge et al., 2002; Grontved et al., 2010; Wang et al.,*
221 *2009*).

222 To clarify the steps of *Pparg* transcription at which TRIM23 acts after activator
223 recruitment, we observed epigenetic changes at the *Pparg* promoters during
224 adipogenesis by ChIP-qPCR analysis. Trimethylation of histone H3 lysine 4
225 (H3K4me3), acetylation of histone H3 lysine 27 (H3K27ac), and monomethylation of
226 histone H4 lysine 20 (H4K20me1) correlate with gene activation and increase at the
227 *Pparg* gene early in the differentiation process, whereas dimethylation of histone H3
228 lysine 9 (H3K9me2) correlates with gene repression and decreases during adipogenesis
229 (*Fujiki et al., 2009; Mikkelsen et al., 2010; Tie et al., 2009; Wakabayashi et al., 2009;*
230 *Wang et al., 2013*). H3K4me3 and H3K27ac levels at *Pparg* gene increased during
231 adipocyte differentiation, and there was little change caused by TRIM23 depletion
232 (Figure 5A, B). There were no differences in H4K20me1 and H3K9me2 levels at day 2
233 between TRIM23-knockdown 3T3-L1 cells and corresponding control cells (Figure
234 5-figure supplement 1). These results indicate that TRIM23 does not affect epigenetic

marks at the *Pparg* promoter. It has also been reported that the *Pparg* promoter is reorganized by ATP-driven nucleosome remodelers and that C/EBP β binding is required for its chromatin opening. Therefore, we monitored chromatin opening using formaldehyde-assisted isolation of regulatory elements (FAIRE) analysis (Giresi *et al.*, 2007). We performed FAIRE analysis at days 0 and 2, and we observed increased chromatin opening around the C/EBP β binding sites on the *Pparg* promoter at day 2, while there was little difference caused by TRIM23 knockdown (Figure 5C). Since PPAR γ by itself enhances the expression of PPAR γ 2 by binding to the *PPRE* at the *Pparg* promoter, we performed ChIP-qPCR analysis with a PPAR γ antibody and found that the occupancy of PPAR γ at the *Pparg* promoter was significantly decreased at day 4 by TRIM23 depletion (Figure 5D). In accordance with the data for PPAR γ , the occupancy of Pol II at the *Pparg* promoter was equally increased at day 2 but was decreased at day 4, although there was little change in the occupancy of MED1 at day 2 and 4 by TRIM23 depletion (Figure 5E, F). Taken together, knockdown of TRIM23 did not affect formation of early enhanceosomes, epigenetic changes, chromatin remodeling, or recruitment of Pol II at the *Pparg* promoter during early adipocyte differentiation, but knockdown of TRIM23 reduced the formation of late enhanceosomes and the recruitment of Pol II during late adipogenic differentiation.

253

254 **TRIM23 does not affect PPAR γ transcriptional activity in HEK293T cells**

It has been reported that a positive feedback loop between C/EBP α and PPAR γ expression supports the maintenance of the differentiated stage (Rosen *et al.*, 2002).

257 Both C/EBP α and PPAR γ binding sites exist at the *Pparg* promoter, and PPAR γ binding
258 sites also exist at the *Cebpa* locus (Farmer, 2006; Nielsen et al., 2008). PPAR γ activates
259 its own expression via direct targeting and/or via C/EBP α binding to the *Pparg*
260 promoter. If transcriptional activity of PPAR γ is directly enhanced by TRIM23,
261 knockdown of TRIM23 should lead to decreased PPAR γ expression. This hypothesis is
262 important to clarify a discontinuity in PPAR γ expression between early and late
263 adipocyte differentiation. To examine whether TRIM23 mediates PPAR γ expression via
264 the transcriptional activity of PPAR γ , we measured the activity using a dual luciferase
265 system. TRIM23 showed slight suppression of PPAR γ 2-mediated transcriptional
266 activity but did not show a dose-dependent relationship (Figure 6A). It has been
267 reported that the transcriptional activity of PPAR γ was modulated by SUMO-1
268 modification and that some TRIM proteins have SUMO E3 activities (Chu and Yang,
269 2011; van Beekum et al., 2009). We therefore investigated whether TRIM23 mediates
270 SUMOylation of PPAR γ 2. Although PPAR γ 2 was definitely SUMOylated in cells,
271 TRIM23 did not affect this modification (Figure 6B). These findings suggest that
272 changes in the transcriptional activity of PPAR γ were not critical for impairment of
273 PPAR γ induction in TRIM23-knockdown cells.

274

275 **TRIM23 knockdown affects the stability of PPAR γ 1 and PPAR γ 2 proteins**

276 To elucidate the mechanism of reduction of PPAR γ expression by TRIM23 knockdown
277 during late adipogenesis, we examined the expression of adipogenic activators during
278 adipocyte differentiation at the protein level. Immunoblot analysis revealed that

279 TRIM23 knockdown did not affect induction of early adipogenic activators but that
280 TRIM23 knockdown impaired induction of late adipogenic activators (Figure 7A).
281 Protein levels of PPAR γ 1 and PPAR γ 2 were already decreased at day 2 by TRIM23
282 knockdown (Figure 7B), whereas mRNA level of PPAR γ 1 was hardly reduced and that
283 of PPAR γ 2 was moderately reduced in TRIM23-knockdown cells (Figure 3). Since the
284 amount of PPAR γ protein was more greatly reduced than the amount of *Pparg* mRNA in
285 TRIM23-knockdown cells, we speculated that the stability of PPAR γ protein was
286 impaired by TRIM23 knockdown. It has been reported that the stability of PPAR γ
287 protein is regulated by the ubiquitin proteasome systems (*Floyd and Stephens, 2002*). To
288 determine whether reduction of PPAR γ protein in TRIM23-knockdown cells depends on
289 proteasome activity, we observed the levels of PPAR γ protein in the presence and
290 absence of a proteasome inhibitor, MG132. 3T3-L1 cells were differentiated for 48 hr
291 and subsequently treated with MG132. Immunoblot analysis showed that administration
292 of MG132 blocked the reduction of both PPAR γ 1 and PPAR γ 2 protein levels in
293 TRIM23-knockdown cells (Figure 7C). We also examined protein levels of PPAR γ in
294 preadipocytes and found that administration of MG132 blocked the reduction of PPAR γ
295 in TRIM23-knockdown cells (Figure 7-figure supplement 1). These findings indicated
296 that the presence of TRIM23 is sufficient to inhibit degradation of PPAR γ not only in a
297 differentiating state but also in an undifferentiated state. Next, we examined the protein
298 stability of PPAR γ 1 and PPAR γ 2. TRIM23-knockdown 3T3-L1 cells and the
299 corresponding control cells were differentiated by the differentiation cocktail for 48 hr,
300 and were subsequently treated with MG132 for 6 hr and with cycloheximide (CHX) for

301 the indicated times. TRIM23 knockdown promoted the degradation of PPAR γ 1 and
302 PPAR γ 2 (Figure 7D, E). These results suggest that TRIM23 stabilized PPAR γ 1 and
303 PPAR γ 2 proteins during adipocyte differentiation.

304

305 **TRIM23 functions as an E3 ubiquitin ligase for PPAR γ 2**

306 Since it has been shown that TRIM23 is a putative E3 ubiquitin ligase and mediates
307 atypical polyubiquitin conjugation to NEMO, we hypothesized that TRIM23 was
308 involved in the stability of PPAR γ protein via its E3 ligase activity (*Arimoto et al.*,
309 2010). We next examined whether TRIM23 binds to and ubiquitinates PPAR γ 2. Using
310 immunoprecipitation assays in HEK293T cells, we detected overexpressed HA-PPAR γ 2
311 in a protein complex with FLAG-TRIM23 (Figure 8A). This interaction was not
312 affected by the treatment of troglitazone (Figure 8B). We also found that endogenous
313 PPAR γ 2 was co-precipitated with FLAG-TRIM23 (Figure 8C). Furthermore, we found
314 that TRIM23 facilitated ubiquitination of PPAR γ 2 *in vivo* and *in vitro* (Figure 8D, E).
315 We next examined which domain of TRIM23 was required for adipocyte differentiation.
316 3T3-L1 cells were infected with a retrovirus expressing shRNA for TRIM23
317 (shTRIM23a) or a non-targeting control shRNA (shControl) and were subsequently
318 infected with a retrovirus expressing control or shRNA-resistant FLAG-TRIM23
319 deletion mutants (Figure 8F). Expression levels of TRIM23 were verified by
320 immunoblot analysis (Figure 8G). These cells were induced to differentiate, and the
321 ability to undergo differentiation to mature adipocytes was evaluated by determination
322 of lipid accumulation using Oil Red O staining. As expected, even a small amount of

323 wild-type TRIM23 expression rescued lipid accumulation; however, a larger amount of
324 TRIM23 deletion mutants failed to rescue lipid accumulation, indicating that both an
325 amino-terminal RING finger domain, which is a ubiquitin ligase catalytic domain, and a
326 carboxy-terminal ARF domain were required for adipocyte differentiation (Figure 8H).
327 These results suggest that ubiquitin conjugation to PPAR γ by TRIM23 plays an
328 important role in adipocyte differentiation.

329

330 **TRIM23 mediates atypical polyubiquitin conjugation, leading to reduced**
331 **recognition by the proteasomal ubiquitin receptor S5a**

332 Degradative polyubiquitin chains are targeted to proteasomes through ubiquitin
333 receptors including S5a/Rpn10 and Rad23. We next examined the binding of
334 ubiquitinated PPAR γ to GST-ubiquitin receptors and found that ubiquitinated PPAR γ
335 purified from cells exogenously expressing TRIM23 bound less efficiently to S5a than
336 did that from cells without exogenous expression of TRIM23. In contrast, HR23B
337 bound to ubiquitinated PPAR γ from both cells with and those without exogenous
338 expression of TRIM23 (Figure 9A). These findings indicate that TRIM23-dependent
339 modification of PPAR γ *in vivo* decreased its recognition by 26S proteasome in a manner
340 dependent on the proteasome subunit S5a/Rpn10. It is well known that K48-linked
341 ubiquitin chains are responsible for proteasomal degradation and that K63-linked chains
342 are involved in various cell signaling processes, though the roles of other atypical
343 ubiquitin linkages through M1, K6, K11, K27, K29 or K33 or mixed linkages within the
344 same chain remain unclear (*Kulathu and Komander, 2012*). We hypothesized that

345 TRIM23 mediates atypical ubiquitination of PPAR γ to inhibit its degradation. We
346 performed an *in vitro* ubiquitination assay using methylated ubiquitin or various
347 ubiquitin mutants (all Lys mutated to Arg except the indicated Lys residue) to study the
348 TRIM23-mediated ubiquitin-linkages of PPAR γ . Intriguingly, TRIM23 mediated
349 ubiquitin conjugation to PPAR γ in the presence of methylated ubiquitin and
350 amino-terminally His₆-tagged no Lys (K0) ubiquitin (Figure 9B). Considering that
351 methylated ubiquitin is unable to form polyubiquitin chains and that amino-terminally
352 His₆-ubiquitin mutants interfere with linear ubiquitin conjugation, these findings
353 indicated that TRIM23 ubiquitinated PPAR γ at multiple sites. Furthermore, TRIM23
354 more efficiently mediated ubiquitin conjugation in the presence of untagged K0
355 ubiquitin or His₆-K27 ubiquitin (Figure 9B), suggesting that TRIM23 can conjugate
356 linear and K27-linked polyubiquitin chains to PPAR γ . To confirm that this atypical
357 ubiquitination of PPAR γ is responsible for reduced recognition by 26S proteasome, we
358 performed an *in vitro* binding assay using PPAR γ ubiquitinated by TRIM23 and
359 GST-ubiquitin receptors including HR23B and S5a. Consistent with the results shown in
360 Figure 9A, although GST-HR23B efficiently bound to M1- and K27-Ub conjugates on
361 PPAR γ 2, GST-S5a poorly pulled down the conjugates (Figure 9C and 9D). Taken
362 together, these findings suggested that atypically ubiquitinated PPAR γ by TRIM23
363 decreased its recognition by 26S proteasome, leading to resistance to proteasomal
364 degradation.

365

366 **Ectopic expression of PPAR γ 2 rescues the adipogenic defect in**

367 **TRIM23-knockdown 3T3-L1 cells**

368 Our data suggest that the defect in adipogenesis by TRIM23 knockdown was caused at
369 least through the decreased expression of PPAR γ 2. Therefore, we expected that
370 overexpression of PPAR γ 2 at an abundance that is sufficient to overcome the instability
371 of PPAR γ 2 protein should rescue the adipogenic defect by TRIM23 knockdown. To
372 confirm this hypothesis, 3T3-L1 cells were infected with a retrovirus expressing shRNA
373 for TRIM23 (shTRIM23a) or a non-targeting control shRNA (shControl) and were
374 subsequently infected with a retrovirus expressing HA-PPAR γ 2 or control. Expression
375 levels of PPAR γ 2 and TRIM23 were verified by immunoblot analysis (Figure 10A and
376 Figure 10-figure supplement 1). TRIM23 knockdown was maintained in spite of ectopic
377 expression of PPAR γ 2 during adipocyte differentiation (Figure 10B). These cells were
378 induced to differentiate, and the ability to undergo differentiation to mature adipocytes
379 was evaluated by the determination of lipid accumulation using Oil Red O staining
380 (Figure 10C) and determination of relative mRNA levels of adipocyte-specific genes
381 (Figure 10D and Figure 10-figure supplement 1). Ectopic expression of PPAR γ 2
382 remarkably rescued lipid accumulation in TRIM23-knockdown cells and the induction
383 of adipocyte-specific genes. The induction of early transcriptional factors, C/EBP β and
384 C/EBP δ , in TRIM23-depleted cells with ectopic expression of PPAR γ 2 was largely
385 rescued to levels comparable to those in control 3T3-L1 cells during adipocyte
386 differentiation, except for sustained high expression level of C/EBP β after day 4 (Figure
387 10-figure supplement 1). These findings suggest that TRIM23 functions in the upstream
388 stage of PPAR γ induction during adipogenesis.

390 **Discussion**

391

392 Adipocyte differentiation is tightly regulated by a complicated transcriptional cascade.
393 PPAR γ plays a central role in the late phase of adipogenesis. Thus, elucidation of the
394 mechanisms that regulate PPAR γ expression is essential for understanding adipocyte
395 differentiation. In this study, we showed that TRIM23 knockdown in preadipocytes
396 results in decreased expression of PPAR γ and a severe defect in late adipogenic
397 differentiation. Ectopic expression of PPAR γ 2 rescues the adipogenic defect induced by
398 TRIM23 knockdown. Therefore, we further investigated the mechanism by which
399 TRIM23 regulates the expression of PPAR γ .

400 A considerable number of studies have shown the importance of transcriptional
401 regulation of *Pparg* gene expression. Early adipogenic activators such as C/EBP β and
402 C/EBP δ provoked by adipogenic stimuli induce low expression levels of PPAR γ 1,
403 PPAR γ 2 and C/EBP α (Ishibashi *et al.*, 2012; Yeh *et al.*, 1995). Then PPAR γ and
404 C/EBP α directly induce each other's high expression level that supports the
405 maintenance of the differentiated stage (Rosen *et al.*, 2002). The binding of activators to
406 enhancer DNA elements promotes the recruitment of GTFs and Pol II to the promoter
407 DNA in order to form a PIC (Lemon and Tjian, 2000; Thomas and Chiang, 2006).
408 Activators also mediate the recruitment of covalent histone-modifying enzymes and
409 ATP-driven nucleosome remodeling complexes to the promoter to reorganize the
410 chromatin architecture to be competent for transcription, leading to transcription
411 initiation (Belotserkovskaya and Berger, 1999; Jaenisch and Bird, 2003; Margueron *et*

412 *al.*, 2005). To elucidate the mechanism of reduced PPAR γ expression by TRIM23
413 knockdown, we investigated the occupancy of activators such as C/EBP β and C/EBP δ ,
414 epigenetic marks by ChIP-qPCR analysis and the degree of chromatin opening by
415 FAIRE analysis at the *Pparg* promoters. However, there were no substantial changes in
416 these during the early phase of differentiation, and we therefore concluded that
417 recruitment of early activators and PIC formation were not affected by TRIM23. An
418 apparent change observed in TRIM23-knockdown cells was a decrease in the
419 occupancy of PPAR γ and Pol II at the *Pparg* locus during the late phase of
420 differentiation, during which PPAR γ and C/EBP α support the high expression level of
421 each other through a positive feedback loop. Therefore, this change caused by TRIM23
422 knockdown was likely to be provoked by impaired positive-feedback regulation of late
423 adipogenic activators.

424 We examined the expression of adipogenic activators in detail, and we found that
425 the protein level of PPAR γ 2 was already decreased at day 2 by TRIM23 knockdown
426 (Figure 7B), whereas the mRNA level of *Pparg* was moderately reduced in
427 TRIM23-knockdown cells (Figure 3). We therefore speculated that TRIM23 regulates
428 PPAR γ expression at the protein level. Although numerous studies have focused on the
429 regulation of *Pparg* expression at the transcriptional level, information on regulation of
430 PPAR γ at the protein level remains limited. The stability of PPAR γ protein is regulated
431 by the ubiquitin proteasome pathway, and PPAR γ is actually an unstable protein ($t_{1/2}$ =2
432 h) (*Christianson et al.*, 2008; *Waite et al.*, 2001). Seven-in-absentia homolog 2 (Siah2)
433 facilitates ubiquitination and degradation of PPAR γ *in vivo*, but it is unclear whether

434 Siah2 directly ubiquitinates PPAR γ *in vitro* (Kilroy *et al.*, 2012). It has also been
435 reported that PPAR γ by itself acts as an E3 ubiquitin ligase and mediates K48-linked
436 polyubiquitination and degradation of p65, suggesting that PPAR γ as an E3 ligase is
437 critical to terminate NF κ B signaling (Hou *et al.*, 2012). PPAR γ forms polyubiquitin
438 chains without a substrate using UBCH3 as E2 *in vitro*, while it has not been determined
439 whether PPAR γ is autoubiquitinated or not. In this study, we showed that TRIM23
440 conjugates atypical polyubiquitin chains including M1- and K27-linked ubiquitin chains
441 to PPAR γ , leading to reduced binding to the proteasomal ubiquitin receptor S5a.
442 Functions regulated by K48- and K63-linked ubiquitin chains have been extensively
443 studied. Past studies have established that K48-linked chains are responsible for
444 proteasomal degradation and that K63-linked chains are involved in various cell
445 signaling processes. Recently, roles of other atypical ubiquitin linkages through K6,
446 K11, K27, K29, K33, M1, or mixed linkages within the same chain have been shown
447 (Kulathu and Komander, 2012). It has been reported that E3 ubiquitin ligase Smad
448 ubiquitination regulatory factor 1 (Smurf1) prevents orphan nuclear receptor Nur77
449 degradation through mediating its atypical ubiquitination via K6 and K27 linkage (Lin
450 *et al.*, 2014). It has also been shown that RING type E3 ligase SCF $^{\beta-TrCP}$ stabilizes the
451 oncoprotein Myc by ubiquitination that requires K33, K48 and K63-linked ubiquitin
452 chains, which antagonizes SCF Fbw7 -mediated K48-linked polyubiquitin chain formation
453 (Popov *et al.*, 2010). Moreover, Ring1B generates self-atypical mixed K6-, K27-, and
454 K48-linked non-proteolytic polyubiquitin chains on itself, whereas E6AP leads to its
455 degradation via ubiquitination of the same residues of Ring1B (Ben-Saadon *et al.*,

456 2006). In this study, we showed that TRIM23 mediates atypical polyubiquitin
457 conjugation including M1- and K27-linked ubiquitin chains to PPAR γ and that
458 ubiquitination of PPAR γ by TRIM23 causes reduced recognition of PPAR γ by 26S
459 proteasome. Although the detailed mechanism remains to be elucidated, these findings
460 suggest that M1- and/or K27-linked polyubiquitin chains to PPAR γ lead to resistance to
461 degradation via reduced recognition by 26S proteasome.

462 In conclusion, TRIM23 is a novel positive regulator of adipocyte maturation via
463 control of switching from early to late adipogenic enhanceosomes through regulating
464 the abundance of PPAR γ (illustrated in Figure 10E). Results of further studies on
465 TRIM23 may be useful for revealing the abnormalities in adipocyte differentiation and
466 for providing a potential therapeutic target for obesity and diabetes mellitus.

467 **Materials and Methods**

468

469 **Mice**

470 All experiments were performed according to the guidelines laid down by the Animal
471 Welfare Committee of Hokkaido University and under institutional approval. For
472 diet-induced obesity, male C57BL/6 mice were fed high-fat diet containing a 57-kcal%
473 fat high-fat diet (Clea Japan, Inc., Tokyo, Japan) for 27 weeks starting at 8 weeks of age
474 (n = 3). Simultaneously, a separate group of male C57BL/6 mice were fed a diet of
475 normal chow (n = 3) containing 5 kcal% fat and served as lean controls. The epididymal
476 fat pads were dissected and minced and then placed in 1 mg/mL collagenase
477 (Sigma-Aldrich, St. Louis, Missouri) in PBS and incubated at 37°C with shaking for 30
478 min. The samples were then centrifuged at 300 x g for 5 min at room temperature. The
479 floating fraction was collected as adipocytes, whereas the precipitated fraction was
480 collected as the stromal vascular fraction (SVF).

481

482 **Cell culture and staining**

483 HEK293T cells were cultured under an atmosphere of 5% CO₂ at 37°C in Dulbecco's
484 modified Eagle's medium (Sigma-Aldrich) supplemented with 10% fetal bovine serum
485 (FBS) (Gibco BRL, Paisley, UK). 3T3-L1 cells were cultured under the same conditions
486 in DMEM with 10% calf serum (CS) (Equitech-Bio Inc., Kerrville, TX). Differentiation
487 into mature adipocytes was induced by exposing the confluent cells to DMEM with
488 10% FBS for 2 days and to a conditioned medium supplemented with 0.5 mM IBMX, 1

489 μ M dexamethasone, and 10 μ g/ml insulin (induction medium) for 2 days. Cells were
490 then incubated in a medium containing 5 μ g/ml insulin. After 2 days, the medium was
491 replaced with a conditioned medium. Subsequently, the conditioned medium was
492 changed regularly every 2 days. Intracellular lipid accumulation was evaluated using Oil
493 Red O staining. 3T3-L1 cells cultured on six-well plates were washed with PBS, fixed
494 for 10 min with 10% formaldehyde in PBS, and stained for 30 min with Oil Red O
495 solution (0.5% Oil Red O (Sigma-Aldrich) in isopropanol with Milli Q (3:2 v/v)). After
496 the cells had been washed twice with 60% isopropanol and twice with PBS, lipid
497 accumulation was evaluated. Intracellular triglyceride content was determined by Lab
498 Assay Triglyceride (WAKO, Osaka, Japan) and normalized to the amounts of total
499 cellular protein determined by a Bio-rad protein assay (Bio-Rad Laboratories Inc.,
500 Hercules, CA) according to each manufacturer's instructions. Culture and differentiation
501 of human primary visceral preadipocytes (Poietics human visceral preadipocytes, Lonza
502 Walkersville Inc., Walkersville, MD, USA) into adipocytes were performed according to
503 the manufacturer's protocol.

504

505 **Cloning of cDNAs and plasmid construction**

506 Human *TRIM23* and mouse *Pparg2* cDNAs were amplified by PCR from HEK293T
507 and 3T3-L1 cDNAs, respectively, by polymerase chain reaction (PCR) with KOD plus
508 (Toyobo, Osaka, Japan). The primers used for the amplification are listed in Table 1.
509 *TRIM23* and *Pparg2* cDNAs were ligated into the p3 \times FLAG vector (Invitrogen,
510 Carlsbad, CA) and the pCGN-HA vector.

511

512 **Transfection, immunoprecipitation, and immunoblot analysis**

513 HEK293T cells were transfected by the calcium phosphate method. After 48 hr, the cells
514 were harvested and lysed in a solution containing 50 mM Tris-HCl (pH 7.4), 150 mM
515 NaCl, 1% Triton X-100, leupeptin (10 µg/ml), 1 mM phenylmethylsulfonyl fluoride,
516 400 µM Na₃VO₄, 400 µM EDTA, 10 mM NaF, and 10 mM sodium pyrophosphate. The
517 cell lysates were centrifuged at 16,000×g for 20 min at 4°C, and the resulting
518 supernatant was incubated with antibodies for 2 hr at 4°C. Protein A-Sepharose
519 (Amersham Biosciences, Piscataway, NJ) that had been equilibrated with the same
520 solution was added to the mixture, which was then rotated for 1 hr at 4°C. The resin was
521 separated by centrifugation, washed five times with ice-cold lysis buffer, and then
522 boiled in SDS sample buffer. Immunoblot analysis was performed with primary
523 antibodies, horseradish peroxidase-conjugated antibodies to mouse or rabbit
524 immunoglobulin G (1:20,000 dilutions, Promega Corporation, Madison, WI) and an
525 enhanced chemiluminescence system (ECL, Amersham Pharmacia). The following
526 primary antibodies were used: anti-FLAG M2 (Sigma-Aldrich), anti-HA (Covance,
527 Princeton, NJ), anti-PPARγ (sc-7273, Santa Cruz Biotechnology, Santa Cruz, CA),
528 anti-TRIM23 (HPA039605, Sigma-Aldrich), anti-β-actin AC15 (Sigma-Aldrich),
529 anti-GAPDH (Ambion), anti-HDAC1 (10E2, Cell Signaling Technology), anti-GST
530 (sc-138, Santa Cruz), anti-Ub (P4D1, sc-8017, Santa Cruz), anti-C/EBPα (sc-61, Santa
531 Cruz), anti-C/EBPβ (sc-150, Santa Cruz) and anti-C/EBPδ (sc-151, Santa Cruz).
532 Nuclear extracts and cytoplasmic S100 fraction were prepared from 3T3-L1 cells

533 according to the method of Dignam *et al.* (Dignam *et al.*, 1983).

534

535 **Retrovirus expression system**

536 A complementary DNA encoding mouse *Pparg2* containing an HA-tag at its amino
537 terminus was subcloned into pQCXIH (Takara, Shiga, Japan), and cDNAs encoding
538 shRNA-resistant human TRIM23 deletion mutants containing a 3×FLAG-tag at their
539 amino-terminus were subcloned into pMSCV-neo (Takara). The resulting vectors were
540 used to transfect Plat-E cells and thereby generate recombinant retroviruses. 3T3-L1
541 cells were infected with the recombinant retroviruses and selected in a medium
542 containing hygromycin B (200 µg/ml, Nacalai Tesque, Kyoto, Japan) or G418 (0.4
543 mg/ml, Nacalai Tesque).

544

545 **Measurement of PPAR γ transcriptional activity using dual-luciferase**

546 Cells were seeded in 24-well plates at 5×10^4 cells per well (HEK293T) and then
547 incubated at 37°C with 5% CO₂ overnight. The peroxisome proliferator-activated
548 receptor response element firefly luciferase reporter plasmid (PPRE–Luc, a kind gift
549 from Bruce M. Spiegelman) and pGL4.74 renilla luciferase (Promega) reporter plasmid
550 were transfected with *Pparg* and/or *TRIM23* expression vectors into HEK293T cells
551 using Fugene HD reagent (Roche, Branchburg, NJ). Transfected cells were incubated in
552 DMEM (Invitrogen) supplemented with 10% charcoal-treated fetal bovine serum
553 (Equitech-Bio) for 24 hr and then incubated with 2 µM troglitazone for 24 hr and
554 harvested, and firefly luciferase and renilla luciferase mRNA were quantified by

555 real-time PCR.

556

557 **RNA interference**

558 pSUPER-retro-puro vector was purchased from OligoEngine (OligoEngine, Seattle,
559 WA). The sequences of short hairpin RNA (shRNA) oligonucleotides are listed in Table
560 1. shRNA for a negative control with no significant homology to any known gene
561 sequences in human and mouse genomes was designed according to a previous report
562 (Gou, et al 2004). Approximately 50% confluent Plat-E cells in 100-mm dishes were
563 transfected with 10 µg pSUPER-retro-puro-shTRIM23-a, shTRIM23-b or control
564 shRNA vector using Fugene HD reagent (Roche). Culture supernatant containing the
565 retrovirus was collected 48 hr after transfection, and retroviral supernatant was added to
566 3T3-L1 cell lines in 100-mm dishes with polybrene (8 mg/ml; Sigma-Aldrich). Cells
567 were cultured with puromycin (5 µg/ml) for 1 week. Human primary visceral
568 preadipocytes in six-well tissue culture plates ($\sim 3.3 \times 10^5$ cells per well) were
569 transfected with 12 nM siRNA targeting human TRIM23 (On-TARGET plus SMART
570 pool, L-006523-00-0005, Dharmacon/Thermo Scientific, Lafayette, CO, USA) or with
571 12 nM ON-TARGETplus Non-targeting Pool (D-001810-10-20, Dharmacon) using
572 Lipofectamine RNAiMAX Transfection Reagent (Invitrogen).

573

574 **Cell proliferation assay**

575 Total cell number per dish was counted during a period of 6 days. 3T3-L1 cells were
576 harvested from the 10-cm dish using 0.25% trypsin (Sigma-Aldrich) and 0.1 mM EDTA,

577 and they were resuspended in a condition medium, followed by staining with 0.4%
578 trypan blue (Sigma-Aldrich). Unstained cells were counted under a light microscope.

579

580 **RNA isolation and real-time PCR**

581 Total RNA was isolated from 3T3-L1 cells using an ISOGEN (Nippon Gene, Tokyo,
582 Japan), with removal of contaminating DNA by a TURBO DNA-Free Kit (Invitrogen),
583 and reverse transcription (RT) was performed by ReverTra Ace (Toyobo, Osaka, Japan).
584 The resulting cDNA was subjected to real-time PCR with a StepOne machine and
585 Power SYBR Green PCR master mix (Applied Biosystems, Foster City, CA). The
586 primers used for the amplification are listed in Table 1. *Gtf2b* transcript was used as an
587 internal control to normalize the mRNA levels of each gene.

588

589 **In vitro ubiquitination assay**

590 Reaction mixtures (each 30 μ l) each containing 40 mM HEPES-NaOH (pH 7.9), 60 mM
591 potassium acetate, 15 mM ATP, 5 mM MgCl₂, 0.5 mM EDTA, 2 mM DTT, E1 (0.1 μ g;
592 Enzo Life Sciences, Farmingdale, New York), E2 (0.5 μ g of His₆-UbcH5B or 0.5 μ g of
593 His₆-UbcH5C), ubiquitin (4 μ g of HA-Ub or 10 μ g of other Ub mutants), TRIM23 (1 μ g
594 of His₆-GST-TRIM23-FLAG or 0.1 μ g of TRIM23-FLAG), and PPAR γ (1 μ g of
595 His₆-GST-PPAR γ or 0.1 μ g of PPAR γ) were incubated for 2 hr at 30°C. The reaction
596 was terminated by the addition of SDS sample buffer containing 4% 2-mercaptoethanol
597 and heating at 95°C for 5 min. Immunoblot analysis was performed with mouse
598 monoclonal antibodies to Anti-FLAG M2 (Sigma-Aldrich), anti-HA (Covance) and

599 anti-PPAR γ (sc-7273, Santa Cruz Biotechnology).

600

601 **GST pull-down assay**

602 HEK293T cells transiently transfected with plasmids encoding FLAG-PPAR γ 2 and/or
603 HA-TRIM23 were harvested and lysed. PPAR γ 2-ubiquitin conjugates were prepared by
604 an *in vitro* ubiquitination assay. GST pull-down assays were performed according to the
605 instructions of the manufacturer (Glutathione Sepharose 4B, GE Healthcare, Uppsala,
606 Sweden). Briefly, 5 μ g of GST (UBPBio, Aurora, CO, USA), GST-S5a (UBPBio) or
607 GST-HR23B (UBPBio) was bound to Glutathione Sepharose beads (20 μ l for each
608 sample) for 1 hr, and the beads were then washed three times and resuspended in
609 ice-cold lysis buffer. HEK293T cell lysates or PPAR γ 2-ubiquitin conjugates were
610 incubated with the beads prebound by GST-tagged proteins for 1 hr at 4°C on a rotating
611 platform. The supernatant was collected as an unbound fraction, and nonspecific
612 binding was removed by washing five times with ice-cold lysis buffer. The bound
613 proteins were eluted by 10 mM reduced glutathione. Samples were separated by
614 SDS-PAGE, followed by immunoblotting using indicated antibodies. Equivalent
615 amounts of bound and unbound fractions were loaded in adjacent lanes.

616

617 **Chromatin immunoprecipitation**

618 Cells (1×10^6) were cross-linked with 0.5 M DSG in PBS for 45 min and 1%
619 formaldehyde in PBS for 10 min at room temperature. Cells were resuspended in a
620 hypotonic buffer (10 mM HEPES-NaOH pH 7.9, 1.5 mM MgCl₂, 10 mM KCl, and 0.5

621 mM DTT) and were homogenized using a dounce homogenizer. Crude nuclei were
622 lysed in lysis buffer (0.1% SDS, 1% Triton X-100, 10 mM EDTA, 150 mM NaCl, 50
623 mM Tris-HCl pH 8.0) and were sonicated with a Bioruptor Sonicator (Diagenode,
624 Sparta, NJ) 30 times for 30 sec each time at the maximum power setting to generate
625 DNA fragments of ~150-400 bps. Sonicated chromatin was incubated for 3 hr at 4°C
626 with 5–15 µg of normal IgG or specific antibodies. Antibodies used were as follows:
627 Normal rabbit IgG (sc-2027, Santa Cruz), Normal mouse IgG (sc-2025, Santa Cruz),
628 anti-Pol II total Rpb1 (F-12, sc-55492, Santa Cruz), anti-C/EBPβ (sc-150, Santa Cruz),
629 anti-C/EBPδ (sc-636, Santa Cruz), anti-PPARγ (sc-1984, Santa Cruz), anti-MED1
630 (sc-5334, Santa Cruz), H3K4me3 (07-473, EMD Millipore, Billerica, MA, USA),
631 H3K27ac (ab4729, Abcam, Cambridge, MA), H3K9me2 (ab1220, Abcam) and
632 H4K20me1 (ab9051, Abcam). Then protein A agarose (GE Healthcare) preblocked with
633 BSA and salmon sperm DNA (BioDynamics Laboratory, Tokyo, Japan) was added and
634 incubated for 1 hr at 4°C. Beads were washed once with IP buffer (20 mM Tris-HCl pH
635 8.0, 150 mM NaCl, 2 mM EDTA, 1% Triton X-100), 2 times with high-salt buffer (20
636 mM Tris-HCl pH 8.0, 500 mM NaCl, 2 mM EDTA, 1% Triton X-100), 2 times with
637 LiCl buffer (250 mM LiCl, 20 mM Tris-HCl pH 8.0, 1 mM EDTA, 1% Triton X-100,
638 0.1% NP40 and 0.5% NaDOC), and two times with TE buffer. Bound complexes were
639 eluted from the beads with 100 mM NaHCO₃ and 1% SDS by incubating at 50°C for 30
640 min with occasional vortexing. Crosslinking was reversed by overnight incubation at
641 65°C. Immunoprecipitated DNA and input DNA were treated with RNase A and
642 Proteinase K by incubation at 45°C. DNA was purified using a QIAquick PCR

643 purification kit (28106, QIAGEN, Valencia, CA) or MinElute PCR purification kit
644 (28006, QIAGEN). Immunoprecipitated and input material was analyzed by
645 quantitative PCR. ChIP signal was normalized to total input.

646

647 **Formaldehyde-assisted isolation of regulatory elements (FAIRE)**

648 3T3-L1 cells (1×10^6) were cross-linked, and crude nuclei were isolated and sonicated
649 as described for the ChIP assay (*Simon et al., 2012*). Samples were centrifuged and
650 DNA in the supernatants was isolated by three extractions with
651 phenol/chloroform/isoamyl alcohol (25:24:1). After the final extraction, the FAIRE
652 samples were reverse cross-linked as described for the ChIP assay. The enrichment of
653 fragmented genomic DNA in the FAIRE samples and input material was analyzed by
654 quantitative PCR. FAIRE signal was normalized to total input.

655

656 **Statistical analysis**

657 We used the unpaired Student's *t* test to determine the statistical significance of
658 experimental data.

659

660 **Acknowledgements**

661 We thank Susanne Mandrup for kindly providing a series of ChIP-qPCR primer
662 sequences, Bruce M. Spiegelman for *PPRE-Luc* reporter plasmid, Toshio Kitamura,
663 Hisato Saito for plasmids and cell lines, Miho Uchiumi and Yuri Soida for help in
664 preparing the manuscript.

665

666 **Funding**

667	<u>Funder</u>	<u>Grant reference number</u>	<u>Author</u>
668	<u>KAKENHI</u>	<u>24112006</u>	<u>Shigetsugu Hatakeyama</u>
669	<u>KAKENHI</u>	<u>24390065</u>	<u>Shigetsugu Hatakeyama</u>
670	<u>KAKENHI</u>	<u>10632424</u>	<u>Masashi Watanabe</u>
671	<u>KAKENHI</u>	<u>25118501</u>	<u>Hidehisa Takahashi</u>
672	The Suzuken Memorial		Shigetsugu Hatakeyama
673	<u>Foundation</u>		
674	<u>The Naito Foundation</u>		<u>Shigetsugu Hatakeyama</u>
675	The Uehara Memorial Foundation		Shigetsugu Hatakeyama
676	<u>Foundation</u>		

677

678 The funders had no role in study design, data collection and interpretation, or the
679 decision to submit the work for publication.

680

681 **Author contributions**

682 MW, Conception and design, Acquisition of data, Analysis and interpretation of data,
683 Drafting or revising the article; HT, Conception and design, Analysis and interpretation
684 of data, Drafting or revising the article; YS, Conception and design, Analysis and
685 interpretation of data, Drafting or revising the article; TO, Acquisition of data, Analysis
686 and interpretation of data; SI, Acquisition of data, Analysis and interpretation of data;
687 MS, Acquisition of data, Analysis and interpretation of data; WM, Acquisition of data,
688 Analysis and interpretation of data; KT, Analysis and interpretation of data, Drafting or
689 revising the article; SH, Conception and design, Analysis and interpretation of data,
690 Drafting or revising the article

691

692 **Ethics**

693 Animal experimentation: All animal protocols were reviewed and approved by the
694 Animal Welfare Committee of Hokkaido University. The work presented in this study is
695 covered by the Animal Protocol Numbers APN-10-0077 and APN13-0040. All
696 researchers, who performed procedures using live animal, were pre-approved by the
697 Animal Welfare Committee of Hokkaido University, based on their completion of
698 required animal use and care training, and acceptable previous experience in animal
699 experiments.

700

701 **References**

702

- 703 Ahmadian, M., J.M. Suh, N. Hah, C. Liddle, A.R. Atkins, M. Downes, and R.M. Evans.
704 2013. PPARgamma signaling and metabolism: the good, the bad and the future.
705 *Nat Med.* **19**:557-566.
- 706 Arimoto, K.I., K. Funami, Y. Saeki, K. Tanaka, K. Okawa, O. Takeuchi, S. Akira, Y.
707 Murakami, and K. Shimotohno. 2010. Polyubiquitin conjugation to NEMO by
708 tripartite motif protein 23 (TRIM23) is critical in antiviral defense. *Proc Natl*
709 *Acad Sci U S A.*
- 710 Barak, Y., M.C. Nelson, E.S. Ong, Y.Z. Jones, P. Ruiz-Lozano, K.R. Chien, A. Koder,
711 and R.M. Evans. 1999. PPAR gamma is required for placental, cardiac, and
712 adipose tissue development. *Mol Cell.* **4**:585-595.
- 713 Belotserkovskaya, R., and S.L. Berger. 1999. Interplay between chromatin modifying
714 and remodeling complexes in transcriptional regulation. *Crit Rev Eukaryot Gene*
715 *Expr.* **9**:221-230.
- 716 Ben-Saadon, R., D. Zaaroor, T. Ziv, and A. Ciechanover. 2006. The polycomb protein
717 Ring1B generates self atypical mixed ubiquitin chains required for its in vitro
718 histone H2A ligase activity. *Mol Cell.* **24**:701-711.
- 719 Boergesen, M., T.A. Pedersen, B. Gross, S.J. van Heeringen, D. Hagenbeek, C.
720 Bindesboll, S. Caron, F. Lalloyer, K.R. Steffensen, H.I. Nebb, J.A. Gustafsson,
721 H.G. Stunnenberg, B. Staels, and S. Mandrup. 2012. Genome-wide profiling of
722 liver X receptor, retinoid X receptor, and peroxisome proliferator-activated
723 receptor alpha in mouse liver reveals extensive sharing of binding sites. *Mol Cell*
724 *Biol.* **32**:852-867.
- 725 Chen, X., H. Xu, P. Yuan, F. Fang, M. Huss, V.B. Vega, E. Wong, Y.L. Orlov, W. Zhang,
726 J. Jiang, Y.H. Loh, H.C. Yeo, Z.X. Yeo, V. Narang, K.R. Govindarajan, B. Leong,
727 A. Shahab, Y. Ruan, G. Bourque, W.K. Sung, N.D. Clarke, C.L. Wei, and H.H.
728 Ng. 2008. Integration of external signaling pathways with the core
729 transcriptional network in embryonic stem cells. *Cell.* **133**:1106-1117.
- 730 Christianson, J.L., S. Nicolero, J. Straubhaar, and M.P. Czech. 2008. Stearoyl-CoA
731 desaturase 2 is required for peroxisome proliferator-activated receptor gamma
732 expression and adipogenesis in cultured 3T3-L1 cells. *J Biol Chem.*

733 **283**:2906-2916.

734 Chu, Y., and X. Yang. 2011. SUMO E3 ligase activity of TRIM proteins. *Oncogene*.
735 **30**:1108-1116.

736 Dignam, J.D., P.L. Martin, B.S. Shastry, and R.G. Roeder. 1983. Eukaryotic gene
737 transcription with purified components. *Methods Enzymol.* **101**:582-598.

738 Eeckhoutte, J., F. Oger, B. Staels, and P. Lefebvre. 2012. Coordinated Regulation of
739 PPARgamma Expression and Activity through Control of Chromatin Structure in
740 Adipogenesis and Obesity. *PPAR Res.* **2012**:164140.

741 Fajas, L., D. Auboeuf, E. Raspe, K. Schoonjans, A.M. Lefebvre, R. Saladin, J. Najib, M.
742 Laville, J.C. Fruchart, S. Deeb, A. Vidal-Puig, J. Flier, M.R. Briggs, B. Staels, H.
743 Vidal, and J. Auwerx. 1997. The organization, promoter analysis, and expression
744 of the human PPARgamma gene. *J Biol Chem.* **272**:18779-18789.

745 Farmer, S.R. 2006. Transcriptional control of adipocyte formation. *Cell Metab.*
746 **4**:263-273.

747 Floyd, Z.E., and J.M. Stephens. 2002. Interferon-gamma-mediated activation and
748 ubiquitin-proteasome-dependent degradation of PPARgamma in adipocytes. *J*
749 *Biol Chem.* **277**:4062-4068.

750 Fujiki, K., F. Kano, K. Shiota, and M. Murata. 2009. Expression of the peroxisome
751 proliferator activated receptor gamma gene is repressed by DNA methylation in
752 visceral adipose tissue of mouse models of diabetes. *BMC Biol.* **7**:38.

753 Galic, S., J.S. Oakhill, and G.R. Steinberg. 2010. Adipose tissue as an endocrine organ.
754 *Mol Cell Endocrinol.* **316**:129-139.

755 Ge, K., M. Guermah, C.X. Yuan, M. Ito, A.E. Wallberg, B.M. Spiegelman, and R.G.
756 Roeder. 2002. Transcription coactivator TRAP220 is required for PPAR gamma
757 2-stimulated adipogenesis. *Nature.* **417**:563-567.

758 Gerstein, M.B., A. Kundaje, M. Hariharan, S.G. Landt, K.K. Yan, C. Cheng, X.J. Mu, E.
759 Khurana, J. Rozowsky, R. Alexander, R. Min, P. Alves, A. Abyzov, N. Addleman,
760 N. Bhardwaj, A.P. Boyle, P. Cayting, A. Charos, D.Z. Chen, Y. Cheng, D. Clarke,
761 C. Eastman, G. Euskirchen, S. Frietze, Y. Fu, J. Gertz, F. Grubert, A. Harmanci, P.
762 Jain, M. Kasowski, P. Lacroute, J. Leng, J. Lian, H. Monahan, H. O'Geen, Z.
763 Ouyang, E.C. Partridge, D. Patacsil, F. Pauli, D. Raha, L. Ramirez, T.E. Reddy,
764 B. Reed, M. Shi, T. Slifer, J. Wang, L. Wu, X. Yang, K.Y. Yip, G.
765 Zilberman-Schapira, S. Batzoglou, A. Sidow, P.J. Farnham, R.M. Myers, S.M.

766 Weissman, and M. Snyder. 2012. Architecture of the human regulatory network
 767 derived from ENCODE data. *Nature*. **489**:91-100.

768 Giresi, P.G., J. Kim, R.M. McDaniell, V.R. Iyer, and J.D. Lieb. 2007. FAIRE
 769 (Formaldehyde-Assisted Isolation of Regulatory Elements) isolates active
 770 regulatory elements from human chromatin. *Genome Res*. **17**:877-885.

771 Grontved, L., M.S. Madsen, M. Boergesen, R.G. Roeder, and S. Mandrup. 2010.
 772 MED14 tethers Mediator to the N-terminal domain of PPAR{gamma} and is
 773 required for full transcriptional activity and adipogenesis. *Mol Cell Biol*.

774 Hatakeyama, S. 2011. TRIM proteins and cancer. *Nat Rev Cancer*.

775 He, A., S.W. Kong, Q. Ma, and W.T. Pu. 2011. Co-occupancy by multiple cardiac
 776 transcription factors identifies transcriptional enhancers active in heart. *Proc*
 777 *Natl Acad Sci U S A*. **108**:5632-5637.

778 Hnisz, D., B.J. Abraham, T.I. Lee, A. Lau, V. Saint-Andre, A.A. Sigova, H.A. Hoke, and
 779 R.A. Young. 2013. Super-enhancers in the control of cell identity and disease.
 780 *Cell*. **155**:934-947.

781 Hou, Y., F. Moreau, and K. Chadee. 2012. PPARgamma is an E3 ligase that induces the
 782 degradation of NFkappaB/p65. *Nat Commun*. **3**:1300.

783 Imai, T., R. Takakuwa, S. Marchand, E. Dentz, J.M. Bornert, N. Messaddeq, O.
 784 Wendling, M. Mark, B. Desvergne, W. Wahli, P. Chambon, and D. Metzger.
 785 2004. Peroxisome proliferator-activated receptor gamma is required in mature
 786 white and brown adipocytes for their survival in the mouse. *Proc Natl Acad Sci*
 787 *U S A*. **101**:4543-4547.

788 Ishibashi, J., Z. Firtina, S. Rajakumari, K.H. Wood, H.M. Conroe, D.J. Steger, and P.
 789 Seale. 2012. An Evi1-C/EBPbeta complex controls peroxisome
 790 proliferator-activated receptor gamma2 gene expression to initiate white fat cell
 791 differentiation. *Mol Cell Biol*. **32**:2289-2299.

792 Jaenisch, R., and A. Bird. 2003. Epigenetic regulation of gene expression: how the
 793 genome integrates intrinsic and environmental signals. *Nat Genet*. **33**
 794 **Suppl**:245-254.

795 Kilroy, G., H. Kirk-Ballard, L.E. Carter, and Z.E. Floyd. 2012. The Ubiquitin Ligase
 796 Siah2 Regulates PPARgamma Activity in Adipocytes. *Endocrinology*.

797 Kulathu, Y., and D. Komander. 2012. Atypical ubiquitylation - the unexplored world of
 798 polyubiquitin beyond Lys48 and Lys63 linkages. *Nat Rev Mol Cell Biol*.

799 **13**:508-523.

800 Lee, J.E., and K. Ge. 2014. Transcriptional and epigenetic regulation of expression
801 during adipogenesis. *Cell Biosci.* **4**:29.

802 Lefterova, M.I., Y. Zhang, D.J. Steger, M. Schupp, J. Schug, A. Cristancho, D. Feng, D.
803 Zhuo, C.J. Stoeckert, Jr., X.S. Liu, and M.A. Lazar. 2008. PPARgamma and
804 C/EBP factors orchestrate adipocyte biology via adjacent binding on a
805 genome-wide scale. *Genes Dev.* **22**:2941-2952.

806 Lemon, B., and R. Tjian. 2000. Orchestrated response: a symphony of transcription
807 factors for gene control. *Genes Dev.* **14**:2551-2569.

808 Lin, H., Q. Lin, M. Liu, Y. Lin, X. Wang, H. Chen, Z. Xia, B. Lu, F. Ding, Q. Wu, and
809 H.R. Wang. 2014. PKA/Smurf1 signaling-mediated stabilization of Nur77 is
810 required for anticancer drug cisplatin-induced apoptosis. *Oncogene.*
811 **33**:1629-1639.

812 Loven, J., H.A. Hoke, C.Y. Lin, A. Lau, D.A. Orlando, C.R. Vakoc, J.E. Bradner, T.I.
813 Lee, and R.A. Young. 2013. Selective inhibition of tumor oncogenes by
814 disruption of super-enhancers. *Cell.* **153**:320-334.

815 Malik, S., and R.G. Roeder. 2010. The metazoan Mediator co-activator complex as an
816 integrative hub for transcriptional regulation. *Nat Rev Genet.* **11**:761-772.

817 Margueron, R., P. Trojer, and D. Reinberg. 2005. The key to development: interpreting
818 the histone code? *Curr Opin Genet Dev.* **15**:163-176.

819 Meroni, G., and G. Diez-Roux. 2005. TRIM/RBCC, a novel class of 'single protein
820 RING finger' E3 ubiquitin ligases. *Bioessays.* **27**:1147-1157.

821 Mikkelsen, T.S., Z. Xu, X. Zhang, L. Wang, J.M. Gimble, E.S. Lander, and E.D. Rosen.
822 2010. Comparative epigenomic analysis of murine and human adipogenesis.
823 *Cell.* **143**:156-169.

824 Moorman, C., L.V. Sun, J. Wang, E. de Wit, W. Talhout, L.D. Ward, F. Greil, X.J. Lu,
825 K.P. White, H.J. Bussemaker, and B. van Steensel. 2006. Hotspots of
826 transcription factor colocalization in the genome of *Drosophila melanogaster*.
827 *Proc Natl Acad Sci U S A.* **103**:12027-12032.

828 Mori, T., H. Sakaue, H. Iguchi, H. Gomi, Y. Okada, Y. Takashima, K. Nakamura, T.
829 Nakamura, T. Yamauchi, N. Kubota, T. Kadowaki, Y. Matsuki, W. Ogawa, R.
830 Hiramatsu, and M. Kasuga. 2005. Role of Kruppel-like factor 15 (KLF15) in
831 transcriptional regulation of adipogenesis. *J Biol Chem.* **280**:12867-12875.

832 Mueller, E., S. Drori, A. Aiyer, J. Yie, P. Sarraf, H. Chen, S. Hauser, E.D. Rosen, K. Ge,
833 R.G. Roeder, and B.M. Spiegelman. 2002. Genetic analysis of adipogenesis
834 through peroxisome proliferator-activated receptor gamma isoforms. *J Biol*
835 *Chem.* **277**:41925-41930.

836 Nielsen, R., L. Grontved, H.G. Stunnenberg, and S. Mandrup. 2006. Peroxisome
837 proliferator-activated receptor subtype- and cell-type-specific activation of
838 genomic target genes upon adenoviral transgene delivery. *Mol Cell Biol.*
839 **26**:5698-5714.

840 Nielsen, R., T.A. Pedersen, D. Hagenbeek, P. Moulos, R. Siersbaek, E. Megens, S.
841 Denissov, M. Borgesen, K.J. Francoijs, S. Mandrup, and H.G. Stunnenberg. 2008.
842 Genome-wide profiling of PPARgamma:RXR and RNA polymerase II
843 occupancy reveals temporal activation of distinct metabolic pathways and
844 changes in RXR dimer composition during adipogenesis. *Genes Dev.*
845 **22**:2953-2967.

846 Oishi, Y., I. Manabe, K. Tobe, K. Tsushima, T. Shindo, K. Fujiu, G. Nishimura, K.
847 Maemura, T. Yamauchi, N. Kubota, R. Suzuki, T. Kitamura, S. Akira, T.
848 Kadowaki, and R. Nagai. 2005. Kruppel-like transcription factor KLF5 is a key
849 regulator of adipocyte differentiation. *Cell Metab.* **1**:27-39.

850 Ozato, K., D.M. Shin, T.H. Chang, and H.C. Morse, 3rd. 2008. TRIM family proteins
851 and their emerging roles in innate immunity. *Nat Rev Immunol.* **8**:849-860.

852 Popov, N., C. Schulein, L.A. Jaenicke, and M. Eilers. 2010. Ubiquitylation of the amino
853 terminus of Myc by SCF(beta-TrCP) antagonizes SCF(Fbw7)-mediated turnover.
854 *Nat Cell Biol.* **12**:973-981.

855 Rosen, E.D., C.H. Hsu, X. Wang, S. Sakai, M.W. Freeman, F.J. Gonzalez, and B.M.
856 Spiegelman. 2002. C/EBPalpha induces adipogenesis through PPARgamma: a
857 unified pathway. *Genes Dev.* **16**:22-26.

858 Rosen, E.D., and O.A. MacDougald. 2006. Adipocyte differentiation from the inside out.
859 *Nat Rev Mol Cell Biol.* **7**:885-896.

860 Siersbaek, R., R. Nielsen, S. John, M.H. Sung, S. Baek, A. Loft, G.L. Hager, and S.
861 Mandrup. 2011. Extensive chromatin remodelling and establishment of
862 transcription factor 'hotspots' during early adipogenesis. *EMBO J.*
863 **30**:1459-1472.

864 Siersbaek, R., A. Rabiee, R. Nielsen, S. Sidoli, S. Traynor, A. Loft, L.L. Poulsen, A.

865 Rogowska-Wrzesinska, O.N. Jensen, and S. Mandrup. 2014. Transcription
 866 Factor Cooperativity in Early Adipogenic Hotspots and Super-Enhancers. *Cell*
 867 *Rep.*

868 Simon, J.M., P.G. Giresi, I.J. Davis, and J.D. Lieb. 2012. Using formaldehyde-assisted
 869 isolation of regulatory elements (FAIRE) to isolate active regulatory DNA. *Nat*
 870 *Protoc.* **7**:256-267.

871 Steger, D.J., G.R. Grant, M. Schupp, T. Tomaru, M.I. Lefterova, J. Schug, E. Manduchi,
 872 C.J. Stoeckert, Jr., and M.A. Lazar. 2010. Propagation of adipogenic signals
 873 through an epigenomic transition state. *Genes Dev.* **24**:1035-1044.

874 Sugii, S., P. Olson, D.D. Sears, M. Saberi, A.R. Atkins, G.D. Barish, S.H. Hong, G.L.
 875 Castro, Y.Q. Yin, M.C. Nelson, G. Hsiao, D.R. Greaves, M. Downes, R.T. Yu,
 876 J.M. Olefsky, and R.M. Evans. 2009. PPARgamma activation in adipocytes is
 877 sufficient for systemic insulin sensitization. *Proc Natl Acad Sci U S A.*
 878 **106**:22504-22509.

879 Tang, Q.Q., T.C. Otto, and M.D. Lane. 2003a. CCAAT/enhancer-binding protein beta is
 880 required for mitotic clonal expansion during adipogenesis. *Proc Natl Acad Sci U*
 881 *S A.* **100**:850-855.

882 Tang, Q.Q., T.C. Otto, and M.D. Lane. 2003b. Mitotic clonal expansion: a synchronous
 883 process required for adipogenesis. *Proc Natl Acad Sci U S A.* **100**:44-49.

884 Thomas, M.C., and C.M. Chiang. 2006. The general transcription machinery and
 885 general cofactors. *Crit Rev Biochem Mol Biol.* **41**:105-178.

886 Tie, F., R. Banerjee, C.A. Stratton, J. Prasad-Sinha, V. Stepanik, A. Zlobin, M.O. Diaz,
 887 P.C. Scacheri, and P.J. Harte. 2009. CBP-mediated acetylation of histone H3
 888 lysine 27 antagonizes Drosophila Polycomb silencing. *Development.*
 889 **136**:3131-3141.

890 Timmers, H.T., and L. Tora. 2005. SAGA unveiled. *Trends Biochem Sci.* **30**:7-10.

891 Tontonoz, P., E. Hu, R.A. Graves, A.I. Budavari, and B.M. Spiegelman. 1994a. mPPAR
 892 gamma 2: tissue-specific regulator of an adipocyte enhancer. *Genes Dev.*
 893 **8**:1224-1234.

894 Tontonoz, P., E. Hu, and B.M. Spiegelman. 1994b. Stimulation of adipogenesis in
 895 fibroblasts by PPAR gamma 2, a lipid-activated transcription factor. *Cell.*
 896 **79**:1147-1156.

897 Tontonoz, P., and B.M. Spiegelman. 2008. Fat and beyond: the diverse biology of

898 PPARgamma. *Annu Rev Biochem.* **77**:289-312.

899 van Beekun, O., V. Fleskens, and E. Kalkhoven. 2009. Posttranslational modifications
900 of PPAR-gamma: fine-tuning the metabolic master regulator. *Obesity (Silver*
901 *Spring)*. **17**:213-219.

902 Waite, K.J., Z.E. Floyd, P. Arbour-Reily, and J.M. Stephens. 2001.
903 Interferon-gamma-induced regulation of peroxisome proliferator-activated
904 receptor gamma and STATs in adipocytes. *J Biol Chem.* **276**:7062-7068.

905 Wakabayashi, K., M. Okamura, S. Tsutsumi, N.S. Nishikawa, T. Tanaka, I. Sakakibara, J.
906 Kitakami, S. Ihara, Y. Hashimoto, T. Hamakubo, T. Kodama, H. Aburatani, and J.
907 Sakai. 2009. The peroxisome proliferator-activated receptor gamma/retinoid X
908 receptor alpha heterodimer targets the histone modification enzyme
909 PR-Set7/Setd8 gene and regulates adipogenesis through a positive feedback loop.
910 *Mol Cell Biol.* **29**:3544-3555.

911 Wang, L., S. Xu, J.E. Lee, A. Baldridge, S. Grullon, W. Peng, and K. Ge. 2013. Histone
912 H3K9 methyltransferase G9a represses PPARgamma expression and
913 adipogenesis. *EMBO J.* **32**:45-59.

914 Wang, W., L. Huang, Y. Huang, J.W. Yin, A.J. Berk, J.M. Friedman, and G. Wang. 2009.
915 Mediator MED23 links insulin signaling to the adipogenesis transcription
916 cascade. *Dev Cell.* **16**:764-771.

917 Whyte, W.A., D.A. Orlando, D. Hnisz, B.J. Abraham, C.Y. Lin, M.H. Kagey, P.B. Rahl,
918 T.I. Lee, and R.A. Young. 2013. Master transcription factors and mediator
919 establish super-enhancers at key cell identity genes. *Cell.* **153**:307-319.

920 Yeh, W.C., Z. Cao, M. Classon, and S.L. McKnight. 1995. Cascade regulation of
921 terminal adipocyte differentiation by three members of the C/EBP family of
922 leucine zipper proteins. *Genes Dev.* **9**:168-181.

923 Zhang, J., M. Fu, T. Cui, C. Xiong, K. Xu, W. Zhong, Y. Xiao, D. Floyd, J. Liang, E. Li,
924 Q. Song, and Y.E. Chen. 2004. Selective disruption of PPARgamma 2 impairs
925 the development of adipose tissue and insulin sensitivity. *Proc Natl Acad Sci U S*
926 *A.* **101**:10703-10708.

927 Zhu, Y., C. Qi, J.R. Korenberg, X.N. Chen, D. Noya, M.S. Rao, and J.K. Reddy. 1995.
928 Structural organization of mouse peroxisome proliferator-activated receptor
929 gamma (mPPAR gamma) gene: alternative promoter use and different splicing
930 yield two mPPAR gamma isoforms. *Proc Natl Acad Sci U S A.* **92**:7921-7925.

931

932

933 **Figure legends**

934

935 **Figure 1.** TRIM23 is expressed during adipocyte differentiation.

936 **(A)** Real-time PCR analysis of mRNA expression of *Trim23* during 3T3-L1
937 differentiation. Total RNA was isolated from 3T3-L1 cells on the indicated days. *Trim23*
938 mRNA was normalized to that of *Gtf2b*. **(B)** Immunoblot analysis of TRIM23 and
939 PPAR γ protein during 3T3-L1 cell differentiation. **(C)** Real-time PCR analysis of
940 mRNA expression of *Trim23* in mouse adipose tissue. *Trim23* mRNA was normalized to
941 that of *Gtf2b*. **(D)** Subcellular localization of TRIM23. Nuclear extracts and cytoplasmic
942 S100 fraction were prepared from 3T3-L1 cells, and immunoblot analysis of TRIM23,
943 HDAC1, and GAPDH was performed.

944

945 **Figure 2.** TRIM23 is required for 3T3-L1 adipocyte differentiation.

946 **(A)** Immunoblot analysis of TRIM23 knockdown before induction of adipogenesis is
947 shown. **(B)** Cells were stained with Oil Red O to visualize the accumulation of lipid
948 droplets at day 6. **(C)** The amounts of intracellular triacylglyceride (TG) were quantified
949 at day 6. **(D)** RNA levels of *Gtf2b* and *Fabp4* were determined by real-time PCR at days
950 0, 2, 4 and 6. Expression level of each gene was normalized to that of the *Gtf2b*. **(E)**
951 Schematic representation of the *Fabp4* gene. The locations of the sequences amplified
952 in the ChIP are shown at the bottom in base pairs relative to the *Fabp4* transcriptional
953 start site. **(F, G and H)** ChIP analysis of PPAR γ **(F)**, MED1 **(G)**, and Pol II **(H)** on the
954 *Fabp4* gene during adipocyte differentiation. Ct values of each ChIP were normalized to

955 that of input. All data represent means \pm s.d. from three independent experiments. The P
956 values for the indicated comparisons were determined by Student's *t* test (*, $P < 0.05$; **, $P < 0.01$).
957

958

959 **Figure 3.** TRIM23 is required for induction of *Pparg1*, *Pparg2* and *Cebpa* but not for
960 induction of *Cebpb* and *Cebpd* during adipogenesis.

961 RNA levels of *Pparg*, *Cebpa*, *Cebpb* and *Cebpd* were determined by real-time PCR at
962 days 0, 2, 4 and 6. Expression level of each gene was normalized to that of the *Gtf2b*.
963 The data represent means \pm s.d. from three independent experiments. The P values for
964 the indicated comparisons were determined using Student's *t*-test (*, $P < 0.05$; **, $P <$
965 0.01).

966

967 **Figure 4.** TRIM23 knockdown does not affect the induction and occupancy of C/EBP β
968 and C/EBP δ at the *Pparg* promoter during adipogenesis.

969 **(A)** RNA levels of *Trim23*, *Cebpb* and *Cebpd* were determined by real-time PCR at 0, 6,
970 12, 24 and 48 hr. Expression level of each gene was normalized to that of *Gtf2b*. **(B)**
971 Schematic representation of the *Pparg* promoters. The locations of the sequences
972 amplified in the ChIP are shown at the bottom in base pairs relative to the *Pparg1* and
973 *Pparg2* transcriptional start sites. **(C)** Occupancy of C/EBP β and C/EBP δ on a subset of
974 target genes at 4 hr. Ct values of each ChIP were normalized to that of input. **(D)** Cell
975 proliferation analysis of 3T3-L1 cells during adipocyte differentiation. 3T3-L1 cells
976 were counted at each time point. The data represent means \pm s.d. from three

977 independent experiments. The P values for the indicated comparisons were determined
978 by Student's *t* test (*, $P < 0.05$; **, $P < 0.01$).

979

980 **Figure 5.** TRIM23 knockdown does not affect the epigenetic marks for activated genes
981 and chromatin opening but decreases the occupancy of Pol II at the *Pparg* promoters.

982 **(A and B)** ChIP analysis of H3K4me3 **(A)** and H3K27ac **(B)** at the *Pparg* promoters
983 during adipocyte differentiation. Ct values of each ChIP were normalized to that of
984 input. **(C)** Formaldehyde-assisted isolation of regulatory elements (FAIRE) analysis
985 during adipocyte differentiation. The enrichment of fragmented genomic DNA in the
986 FAIRE samples was analyzed and normalized to that of input. **(D, E and F)** ChIP
987 analysis of PPAR γ **(D)**, MED1 **(E)**, and Pol II **(F)** at the *Pparg* promoter during
988 adipocyte differentiation. Ct values of each ChIP were normalized to that of input. All
989 data represent means \pm s.d. from three independent experiments. The P values for the
990 indicated comparisons were determined by Student's *t* test (*, $P < 0.05$; **, $P < 0.01$).

991

992 **Figure 6.** TRIM23 does not affect PPAR γ 2 transcriptional activity.

993 **(A)** TRIM23 does not affect PPAR γ -mediated transcriptional activity in HEK293T cells.
994 The peroxisome proliferator-activated receptor response element firefly luciferase
995 reporter vector (*PPRE-Luc*), pGL4.74 renilla luciferase reporter plasmid, and
996 expression vectors encoding *TRIM23* and *Pparg* were transfected into HEK293T cells
997 and the cells were incubated in culture medium containing 10% charcoal-treated fetal
998 bovine serum for 24 hr. Cells were incubated with or without troglitazone (2 μ M) for 24

999 hr, harvested, and quantified firefly luciferase and renilla luciferase mRNA with
1000 real-time PCR. The data represent means \pm s.d. from three independent experiments. **(B)**
1001 TRIM23 does not promote SUMOylation of PPAR γ 2. An *in vivo* assay for
1002 SUMOylation of PPAR γ 2 by TRIM23 was performed. Expression vectors encoding
1003 FLAG-PPAR γ 2, Myc-TRIM23, and HA-SUMO1 were transfected into HEK293T cells.
1004 Cell lysates were immunoprecipitated with anti-FLAG antibody and then immunoblot
1005 analysis was performed to detect modifications of PPAR γ 2.

1006

1007 **Figure 7.** TRIM23 stabilizes PPAR γ 2.

1008 **(A)** Immunoblot analysis of C/EBP α , C/EBP β , C/EBP δ and PPAR γ protein during
1009 3T3-L1 cell differentiation. **(B)** The intensity of the immunoreactive bands of PPAR γ 2
1010 obtained by immunoblot analysis with anti-PPAR γ antibody was determined relative to
1011 that obtained with anti- β -actin antibody. **(C)** Immunoblot analysis of PPAR γ protein in
1012 the absence and presence of MG132. 3T3-L1 cells with stable knockdown of TRIM23
1013 or the corresponding control cells were differentiated by the differentiation cocktail for
1014 48 hr and subsequently treated with 10 μ M of MG132 for 6 hr. **(D)** 3T3-L1 cells with
1015 stable knockdown of TRIM23 or the corresponding control cells were differentiated by
1016 the differentiation cocktail for 48 hr and subsequently treated with 10 μ M of MG132 for
1017 6 hr, followed by cycloheximide (CHX) treatment (5 μ M) for 0, 1, 2 or 4 hr. The cell
1018 lysates were subjected to immunoblot analysis with an anti-PPAR γ , anti-TRIM23 or
1019 anti- β -actin antibody. β -actin is shown as a loading control. The result is representative
1020 of two independent experiments. **(E)** The intensity of the PPAR γ 1 and PPAR γ 2 bands

1021 was normalized to that of the corresponding β -actin bands shown in **(D)** and is indicated
1022 as a percentage of the normalized value at 0 hr.

1023

1024 **Figure 8.** TRIM23 interacts with PPAR γ 2 and promotes ubiquitination of PPAR γ 2.

1025 **(A)** *In vivo* assay for interaction between TRIM23 and PPAR γ 2. FLAG-TRIM23 and
1026 HA-PPAR γ 2 were transfected into HEK293T cells. Lysates were immunoprecipitated
1027 with anti-FLAG antibody and immunoblotted with anti-FLAG and anti-HA antibodies.

1028 **(B)** *In vivo* assay for interaction between TRIM23 and PPAR γ 2 with or without
1029 troglitazone (1 μ M). FLAG-TRIM23 and HA-PPAR γ 2 were transfected into HEK293T
1030 cells. Coimmunoprecipitation assays were performed using the cell extract from these

1031 cells with anti-FLAG antibody in the presence or absence of 1 μ M troglitazone. **(C)** *In*
1032 *vivo* assay for interaction between TRIM23 and PPAR γ 2. 3T3-L1 cells stably
1033 expressing FLAG-TRIM23 were generated, differentiated, and harvested at day 6.

1034 Whole cell lysates were immunoprecipitated with anti-FLAG antibody and then
1035 immunoblot analysis was performed with anti-FLAG and anti-PPAR γ antibodies. **(D)** *In*

1036 *vivo* assay for ubiquitination of PPAR γ 2 by TRIM23. FLAG-PPAR γ 2, Myc-TRIM23,
1037 and HA-ubiquitin (HA-Ub) were transfected into HEK293T cells. Cell lysates were

1038 immunoprecipitated with anti-FLAG antibody and then immunoblot analysis was
1039 performed to detect ubiquitination of PPAR γ 2. **(E)** Promotion of *in vitro* PPAR γ 2

1040 polyubiquitination by TRIM23. An *in vitro* ubiquitination assay was performed with the
1041 indicated combinations of ATP, HA-Ub, His₆-E1, His₆-E2 (UbcH5B),

1042 His₆-GST-TRIM23-FLAG, and GST-PPAR γ 2. Reaction mixtures were subjected to

1043 immunoblot analysis with anti-PPAR γ (top), anti-HA (middle) or anti-FLAG (bottom).
 1044 The positions of GST-PPAR γ 2 or His₆-GST-TRIM23-FLAG modified by various
 1045 numbers of HA-Ub moieties are indicated. **(F)** Schematic representation of TRIM23
 1046 deletion mutants is shown. Protein motifs are indicated. RING, ring-finger domain;
 1047 B-box, B-box domain; CC, coiled-coil domain; ARF, ADP ribosylation factor domain.
 1048 **(G)** Immunoblot analysis of ectopic expression of TRIM23 deletion mutants in
 1049 TRIM23-knockdown 3T3-L1 cells before induction of adipogenesis. **(H)** Cells were
 1050 stained with Oil Red O to visualize the accumulation of lipid droplets at day 6.
 1051
 1052 **Figure 9.** TRIM23 mediates atypical polyubiquitin conjugation of PPAR γ 2, leading to
 1053 reduced recognition of ubiquitinated PPAR γ 2 by the proteasomal ubiquitin receptor S5a.
 1054 **(A)** PPAR γ 2 polyubiquitination by TRIM23 leads to reduced recognition by the
 1055 proteasomal ubiquitin receptor S5a. HEK293T cells transiently transfected with
 1056 plasmids encoding FLAG-PPAR γ 2 and/or HA-TRIM23 were lysed. GST, GST-HR23B,
 1057 and GST-S5a were resuspended with cell lysates, followed by pull-down with
 1058 glutathione Sepharose beads. Samples were separated by SDS-PAGE, followed by
 1059 immunoblotting using the indicated antibodies. **(B)** *In vitro* PPAR γ 2 polyubiquitination
 1060 by TRIM23. An *in vitro* ubiquitination assay was performed with the indicated
 1061 combinations of ATP, various ubiquitin mutants, His₆-E1, E2 (UbcH5C),
 1062 His₆-GST-TRIM23-FLAG, and GST-PPAR γ 2. Reaction mixtures were subjected to
 1063 immunoblot analysis with anti-PPAR γ (top), anti-TRIM23 (middle) or anti-Ub (bottom)
 1064 antibodies. The positions of GST-PPAR γ 2 or His₆-GST-TRIM23-FLAG modified by

1065 various numbers of ubiquitin moieties are indicated. **(C and D)** Conjugation of PPAR γ 2
1066 with M1- and/or K27-linked polyubiquitin chains leads to reduced recognition by the
1067 proteasomal ubiquitin receptor S5a. An *in vitro* ubiquitination assay was performed with
1068 the indicated combinations of ATP, ubiquitin mutants, His₆-E1, E2 (UbcH5C),
1069 TRIM23-FLAG, and PPAR γ 2. Reaction mixtures were subjected to GST pull-down
1070 assay. PPAR γ 2-ubiquitin conjugates were incubated with GST-S5a (C) or GST-HR23B
1071 (D) prebound to glutathione Sepharose beads. Samples were separated by SDS-PAGE,
1072 followed by immunoblotting using a PPAR γ antibody. Equivalent amounts of bound and
1073 unbound fractions were loaded in each lane.

1074

1075 **Figure 10.** PPAR γ 2 expression rescues the adipogenesis defect in TRIM23-knockdown
1076 3T3-L1 cells.

1077 **(A)** Immunoblot analysis of ectopic PPAR γ 2 expression before induction of
1078 adipogenesis is shown. **(B)** Changes in *Trim23* mRNA during adipocyte differentiation
1079 in 3T3-L1 cells. Total RNA was isolated from 3T3-L1 cells on the indicated days of
1080 differentiation. *Trim23* mRNA was determined by real-time PCR and normalized to that
1081 of *Gtf2b*. **(C)** Cells were stained with Oil Red O to visualize the accumulation of lipid
1082 droplets at day 6. **(D)** RNA levels of *Fabp4*, *Cebpa*, and *Pparg* were determined by
1083 real-time PCR at days 0, 2, 4 and 6 of differentiation. Expression level of each gene was
1084 normalized to the level of *Gtf2b*. The data represent means \pm s.d. from three
1085 independent experiments. The P values for the indicated comparisons were determined
1086 using Student's *t*-test (* $p < 0.05$; ** $p < 0.01$). **(E)** Model for TRIM23 function in

1087 PPAR γ abundance during adipocyte maturation. Several adipogenic stimuli activate
1088 early adipogenic activators such as C/EBP β , C/EBP δ , glucocorticoid receptor (GR) and
1089 signal transducer and activator of transcription 5a (STAT5a). These activators then
1090 induce late adipogenic activators including PPAR γ and C/EBP α . TRIM23 mediates
1091 atypical polyubiquitin conjugation to PPAR γ and may stabilize the PPAR γ protein.
1092 TRIM23 plays a critical role in the switching from early to late adipogenic
1093 enhanceosomes by regulating the abundance of PPAR γ .
1094

1095 **Table 1 List of SYBR Green primers for real-time PCR**

PCR primers for cloning of cDNA		
Gene	Forward primer	Reverse primer
<i>Trim23</i>	AGGATGGCTACCCTGGTTGTAAAC	AAATCAAGCAACATCCAATACT CC
<i>Pparg2</i>	GTTATGGGTGAAACTCTGGGA	CTGCTAATACAAGTCCTTGTA
Oligonucleotides for shRNA		
<i>shTRIM23a</i>	GATCCCCGAAGAAATGGCTCTAAG TGTTCAAGAGACACTTAGAGCCAT TTCTTCTTTTAA	AGCTTAAAAAGAAGAAATGGC TCTAAGTGTCTCTTGAACACTT AGAGCCATTCTTCGGG
<i>shTRIM23b</i>	GATCCCCGGTAGATGTTAAATCGCA TTTCAAGAGAATGCGATTAAACATC TACCTTTTAA	AGCTTAAAAAGGTAGATGTTAA ATCGCATTCTCTTGAAATGCGAT TTAACATCTACCGGG
qRT-PCR primers for gene expression		
<i>Adipoq</i>	GCACTGGCAAGTTCTACTGCAA	GTAGGTGAAGAGAACGGCCTT GT
<i>Cebpa</i>	TGCGCAAGAGCCGAGATAA	CGGTCATTGTCACTGGTCAACT
<i>Cebpb</i>	CAAGCTGAGCGACGAGTACA	AGCTGCTCCACCTTCTTCTG
<i>Cebpd</i>	ATCGACTTCAGCGCCTACAT	GCTTTGTGGTTGCTGTTGAA
<i>Cidec</i>	AGCTAGCCCTTTCCCAGAAG	TCAGGCAGCCAATAAAGTCC
<i>Fabp4</i>	CATCAGCGTAAATGGGGATT	GTCGTCTGCGGTGATTTCAT
<i>Klf15</i>	CCCAATGCCGCCAAACCTAT	GAGGTGGCTGCTCTTGGTGTAC ATC
<i>Pparg1+2</i>	TGCAGGAGCAGAGCAAAGAG	CGGCTTCTACGGATCGAAAC
<i>Pparg1</i>	TGAAAGAAGCGGTGAACCACTG	TGGCATCTCTGTGTCAACCATG
<i>Pparg2</i>	TGGCATCTCTGTGTCAACCATG	GCATGGTGCCTTCGCTGA
<i>Retn</i>	TTTTCTTCCTTGTCCTGAACTG	GATCTTCTTGTCGATGGCTTCAT
<i>Gtf2b</i>	GTTCTGCTCCAACCTTTGCCT	TGTGTAGCTGCCATCTGCACTT
<i>Trim23</i>	TTGGAATGGCTCACACAGAAC	ACATGGGCATCAACAACAC
qPCR primers for ChIP		
<i>Pparg1 -1.0 kb</i>	CTGTCTATCATGTGGGCTTCAG	ACCTTACACATAGGGTGGAGA
<i>Pparg1 -0.4 kb</i>	ACAAACTTCTCCATGACAGACA	CGCCTTGCTCCTCACAG
<i>Pparg1 +0.3kb</i>	CTGCGTAACTGACAGCCTAAC	ACTTGGTCACTCTCCGTCCT
<i>Pparg2 -1.0 kb</i>	GATACACTGCCCTGTGTAAAGG	GAGCAGCCCTTGTCACATAA

<i>Pparg2</i> -0.2 kb	GAACAGTGAATGTGTGGGTCA	CTGACTGAGAGCCAGTTGTGA
<i>Pparg2</i> +0.5kb	GTGAGCATTTTCAGAACACTTGG	GCCTGAAGAAGAACAGAAATT CTAC
<i>Negative control</i>	TGGTAGCCTCAGGAGCTTGC	ATCCAAGATGGGACCAAGCTG
<i>Myog</i>	GGGTCTCTTCCTCTTACCCGAT	ACCTTGCTGGCCATGGAC
<i>Iqck</i>	GAAACAAAGCCTTCCCATCC	TCCTTTCTTGCTGTGGCTTC
<i>Cav2</i>	CTCAGAAAAGGCAGGGAAAG	CCCAGTCATGACAACACCAA
<i>Fabp4</i> -10000 bp	CCATGAGGAAATTCGCTACAC	CCTTCCACCCCTTATCTCACAC
<i>Fabp4</i> -5500 bp	GAGAGCAAATGGAGTTCCCAGA	TTGGGCTGTGACACTTCCAC
<i>Fabp4</i> -200 bp	CATTGCCAGGGAGAACCAA	TCCTTCATGACCAGACCCTGT
<i>Fabp4</i> +500 bp	CAGGTGAACCCGCAAGAAAG	GCTTGGCAAAGAAGGCCAC

1096

1097

1098 **Figure supplement titles and captions**

1099

1100 **Figure 2-figure supplement 1.** Quantitative analysis of *Trim23*, *Cidec*, *Klf15*, *Adipoq*
1101 and *Retn* mRNA during 3T3-L1 differentiation.

1102 mRNA levels of *Trim23*, *Cidec*, *Klf15*, *Adipoq* and *Retn* were determined by real-time
1103 PCR at days 0, 2, 4, and 6. Expression level of each gene was normalized to the level of
1104 *Gtf2b*.

1105

1106 **Figure 2-figure supplement 2.** TRIM23 is required for human visceral preadipocyte
1107 differentiation.

1108 Short interfering RNAs targeting TRIM23 (siTRIM23) and a non-targeting control
1109 siRNA (siControl) were introduced into human primary visceral preadipocytes, and the
1110 preadipocytes were differentiated to mature adipocytes. Adipocytes were stained with
1111 Oil Red O to visualize the accumulation of lipid droplets at day 10.

1112

1113 **Figure 5-figure supplement 1.** Depletion of TRIM23 does not affect H3K9me2 and
1114 H4K20me1 marks at the *Pparg* promoter.

1115 **(A)** Control IgG ChIP does not occupy a subset of gene promoters during adipogenesis.
1116 Ct values of each ChIP were normalized to that of input. **(B and C)** ChIP analysis of
1117 H3K9me2 (B) and H4K20me1 (C) at the *Pparg* promoter during adipocyte
1118 differentiation. Ct values of each ChIP were normalized to that of input. All data
1119 represent means \pm s.d. from three independent experiments. The P values for the

1120 indicated comparisons were determined by Student's *t* test (*, $P < 0.05$; **, $P < 0.01$).

1121

1122 **Figure 7 figure-supplement 1.** The presence of TRIM23 is sufficient to inhibit basal
1123 degradation of PPAR γ .

1124 Immunoblot analysis of PPAR γ protein in the absence and presence of MG132. 3T3-L1
1125 preadipocytes with stable knockdown of TRIM23 or the corresponding control cells
1126 were treated with MG132 (10 mM) for 6 hr.

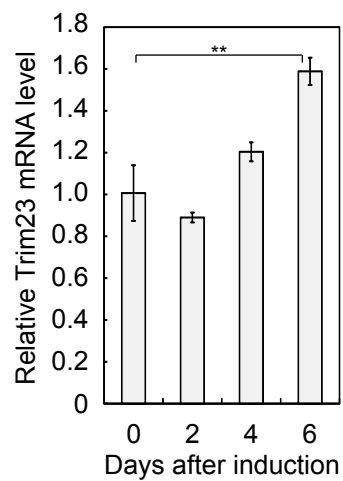
1127

1128 **Figure 10-figure supplement 1.** PPAR γ 2 expression rescues the adipogenesis defect
1129 that occurred in TRIM23-knockdown 3T3-L1 cells.

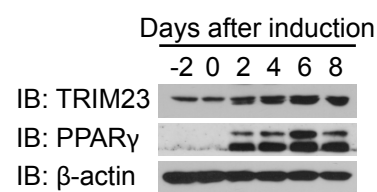
1130 **(A)** Immunoblot analysis of PPAR γ and C/EBP α protein during 3T3-L1 differentiation.

1131 **(B)** RNA levels of *Cidec*, *Klf15*, *Cebpb*, *Adipoq*, *Retn* and *Cebpd*, were determined by
1132 real-time PCR at days 0, 2, 4, and 6. Expression level of each gene was normalized to
1133 that of *Gtf2b*. The data represent means \pm s.d. from three independent experiments. The
1134 P values for the indicated comparisons were determined using Student's *t*-test (* $p <$
1135 0.05; ** $p < 0.01$).

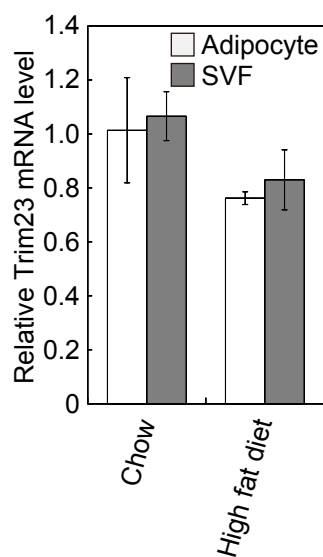
A



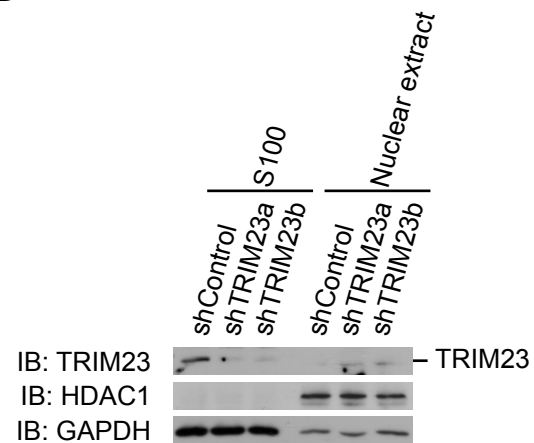
B

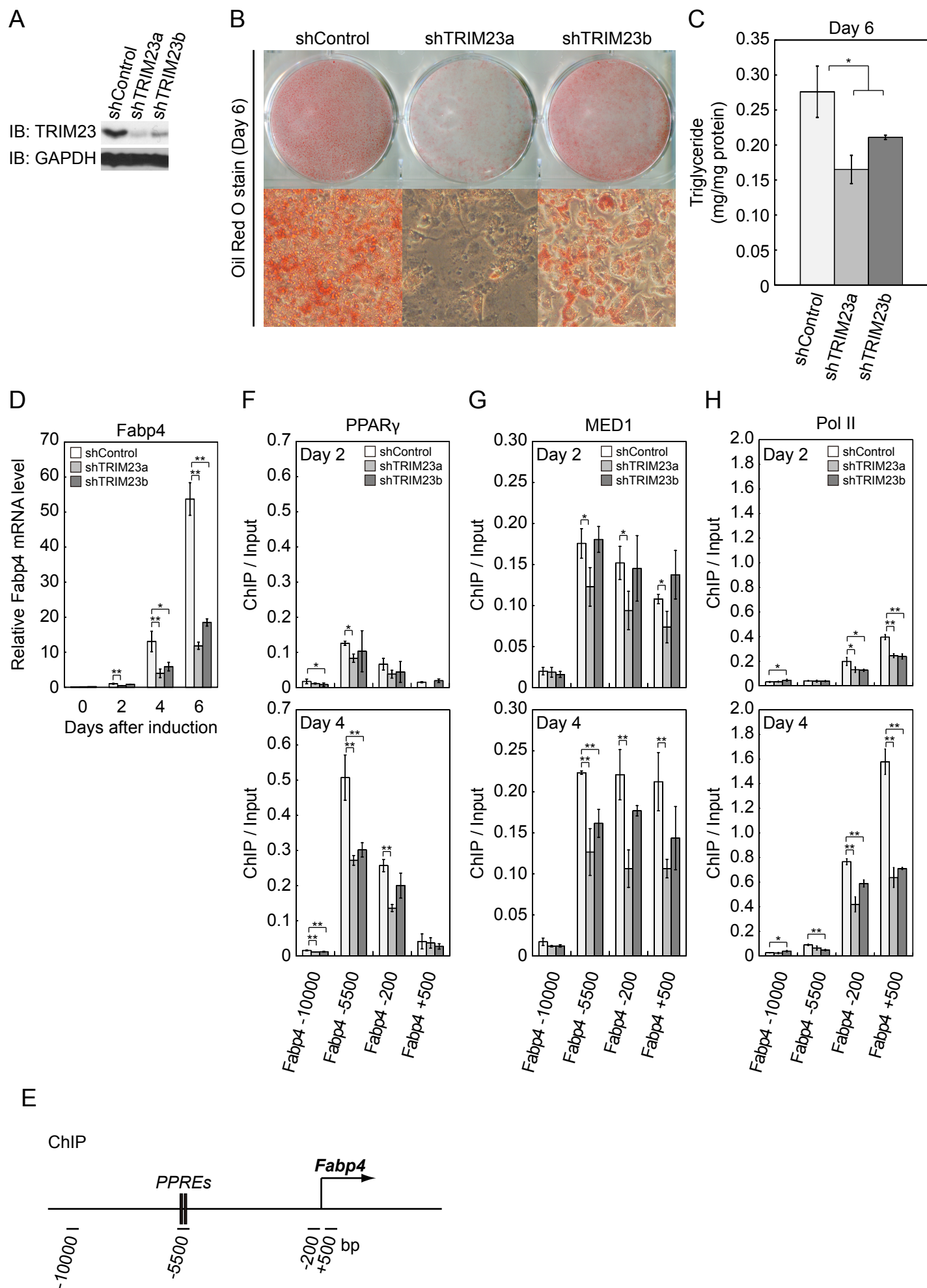


C

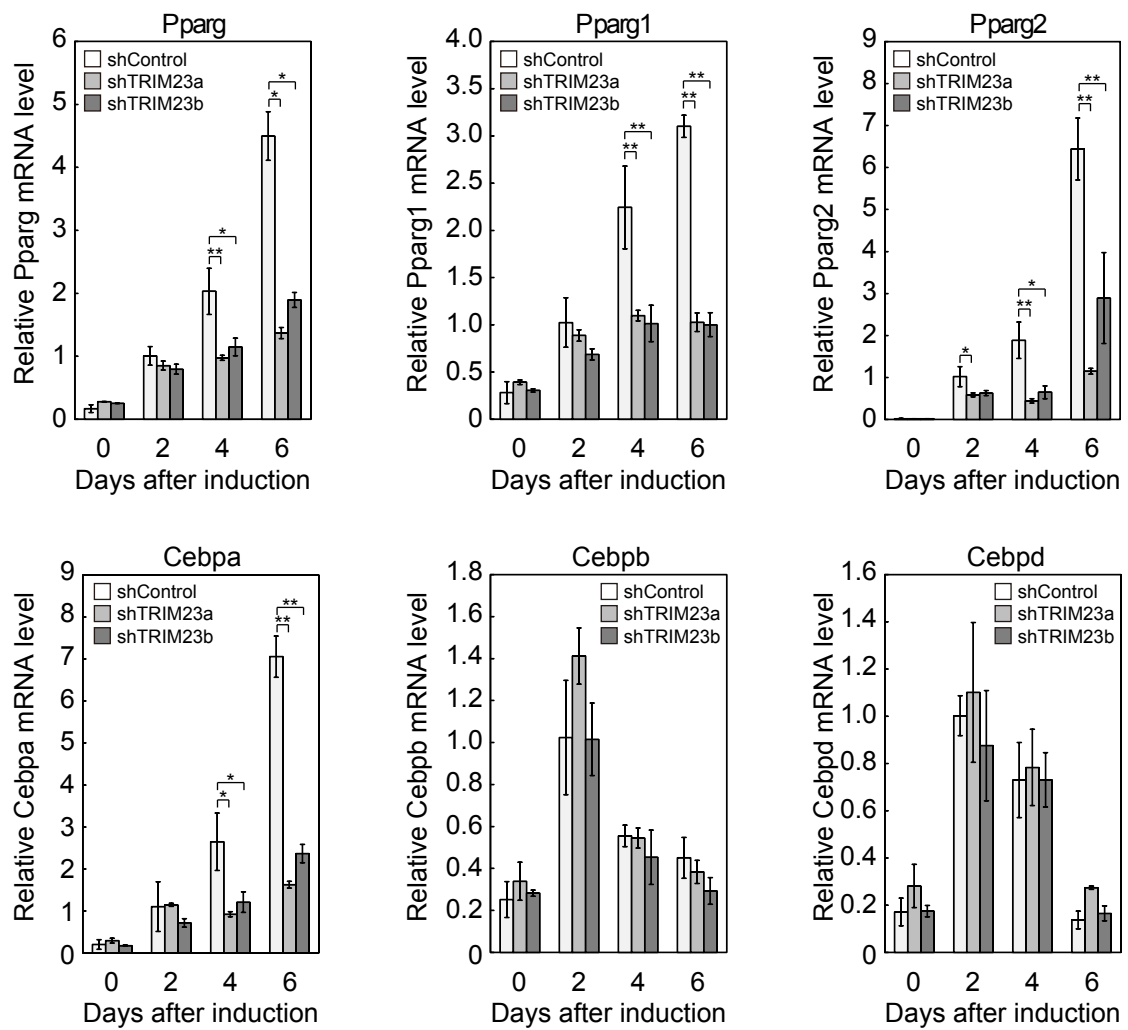


D

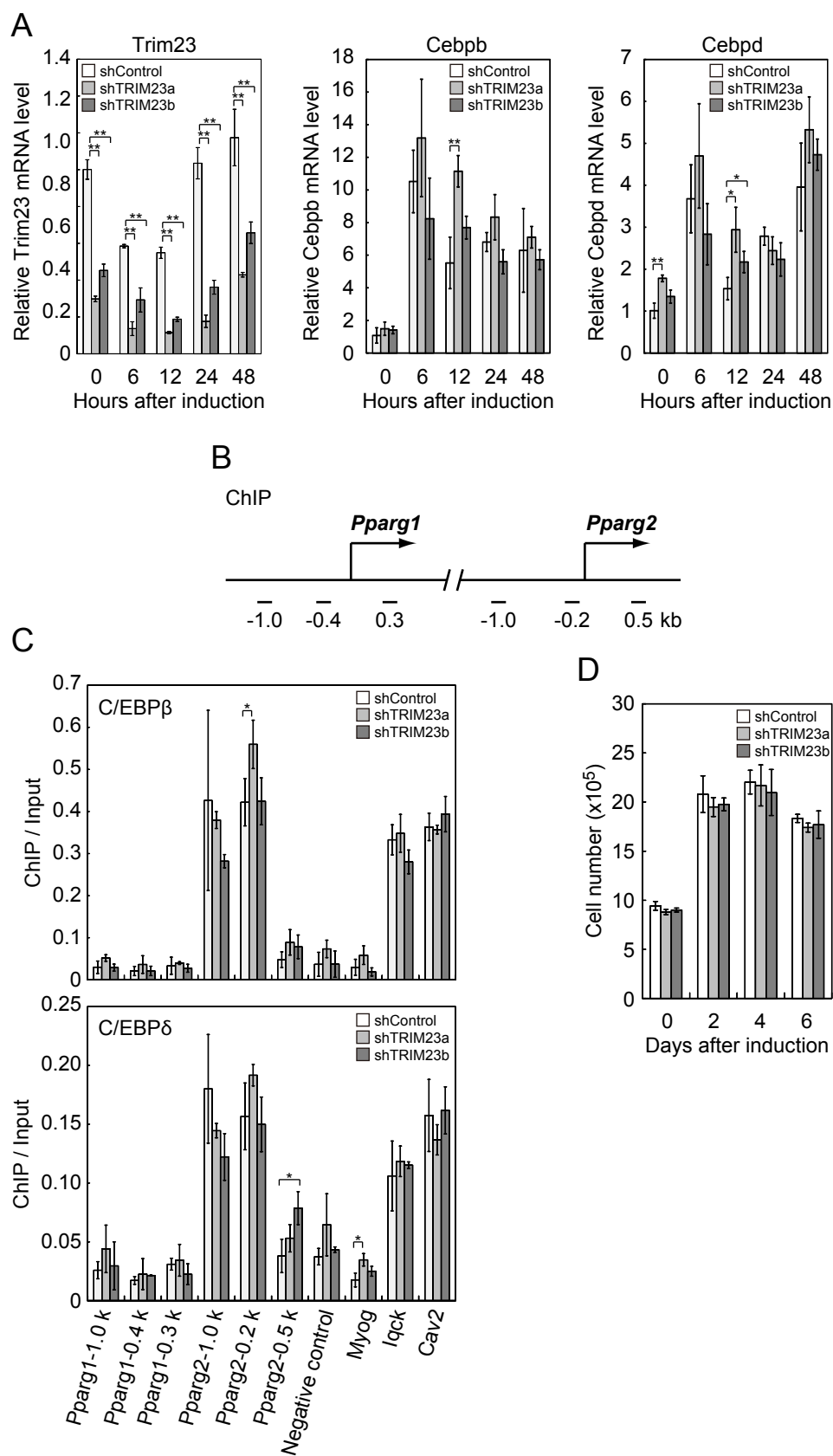




Watanabe, Figure 2

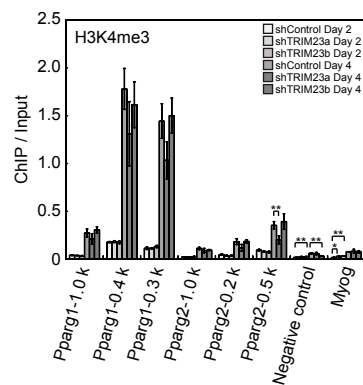


Watanabe, Figure 3

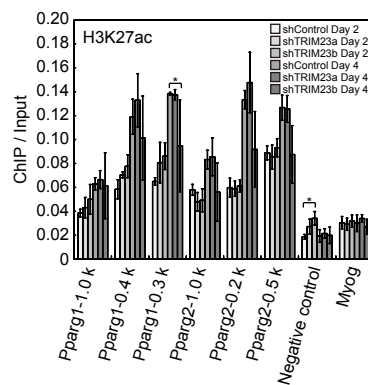


Watanabe, Figure 4

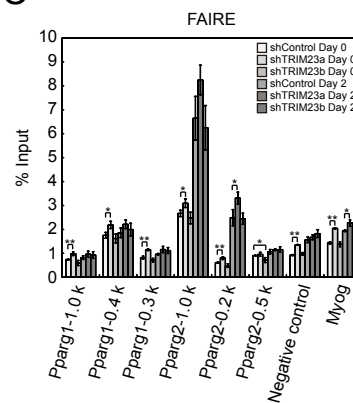
A



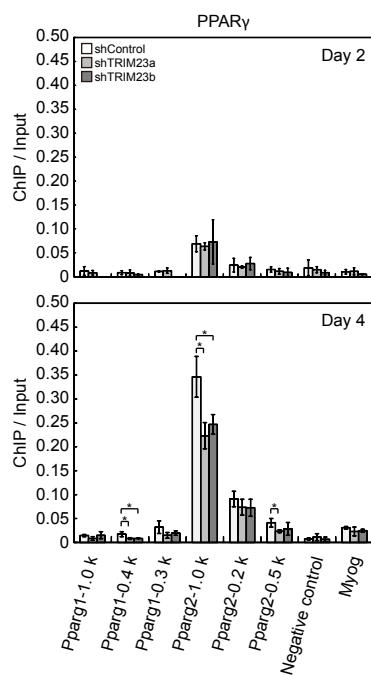
B



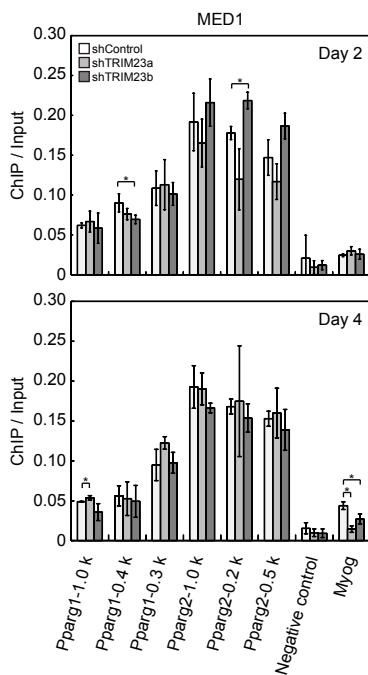
C



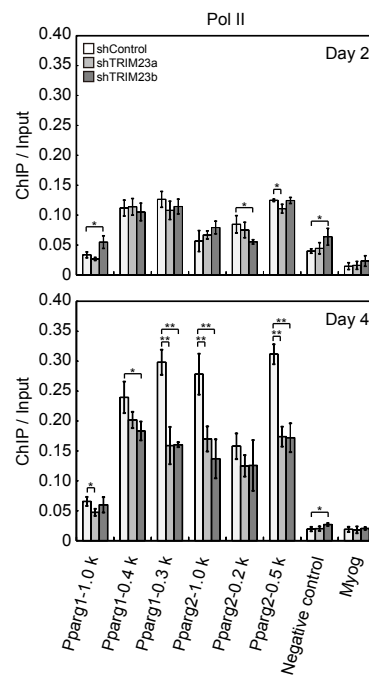
D



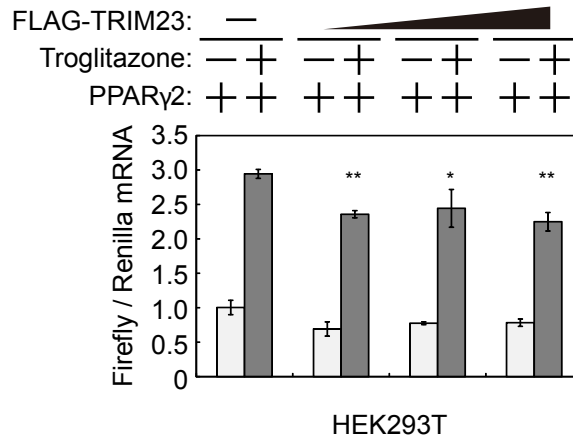
E



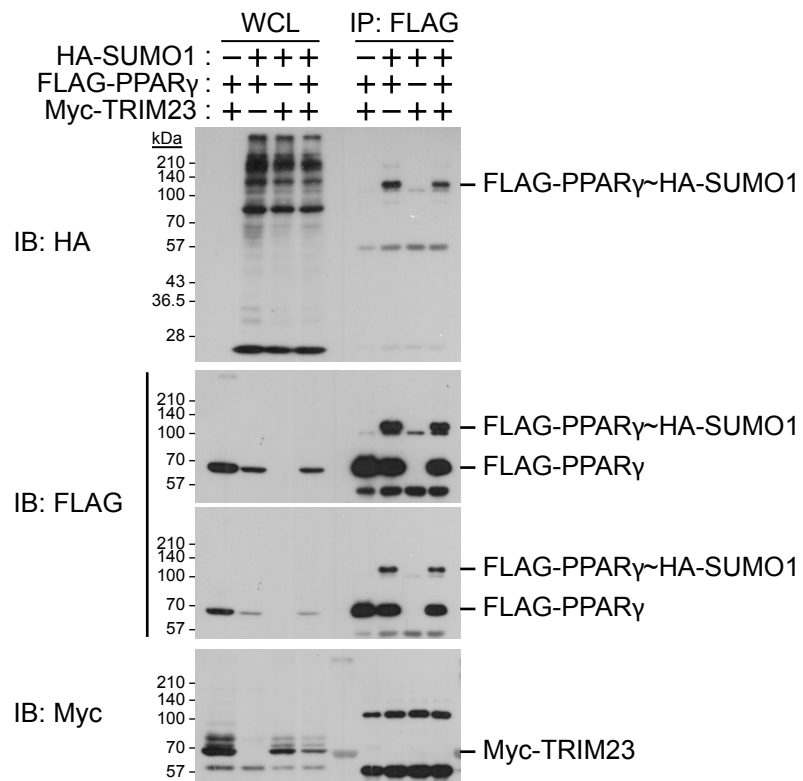
F

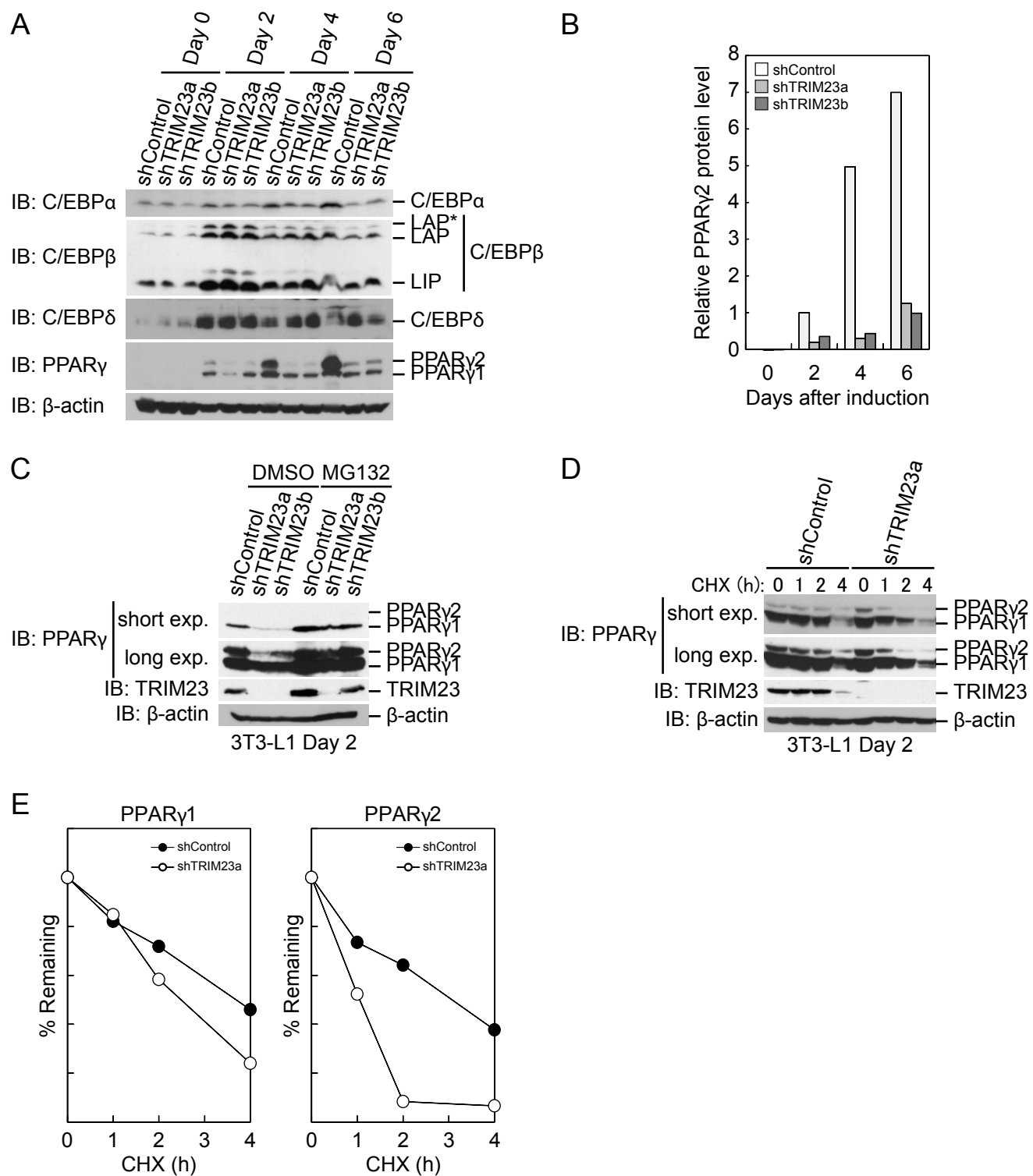


A

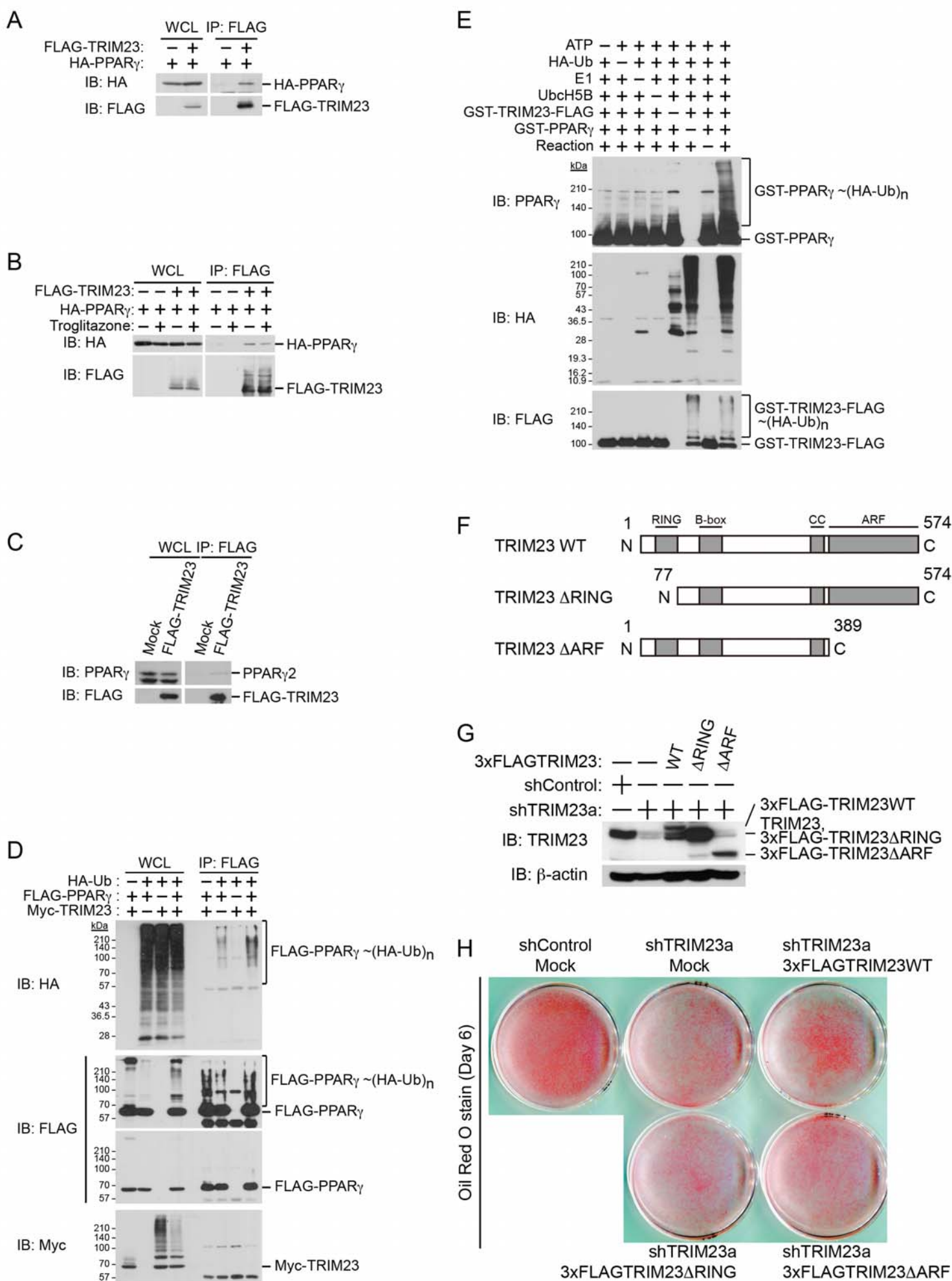


B

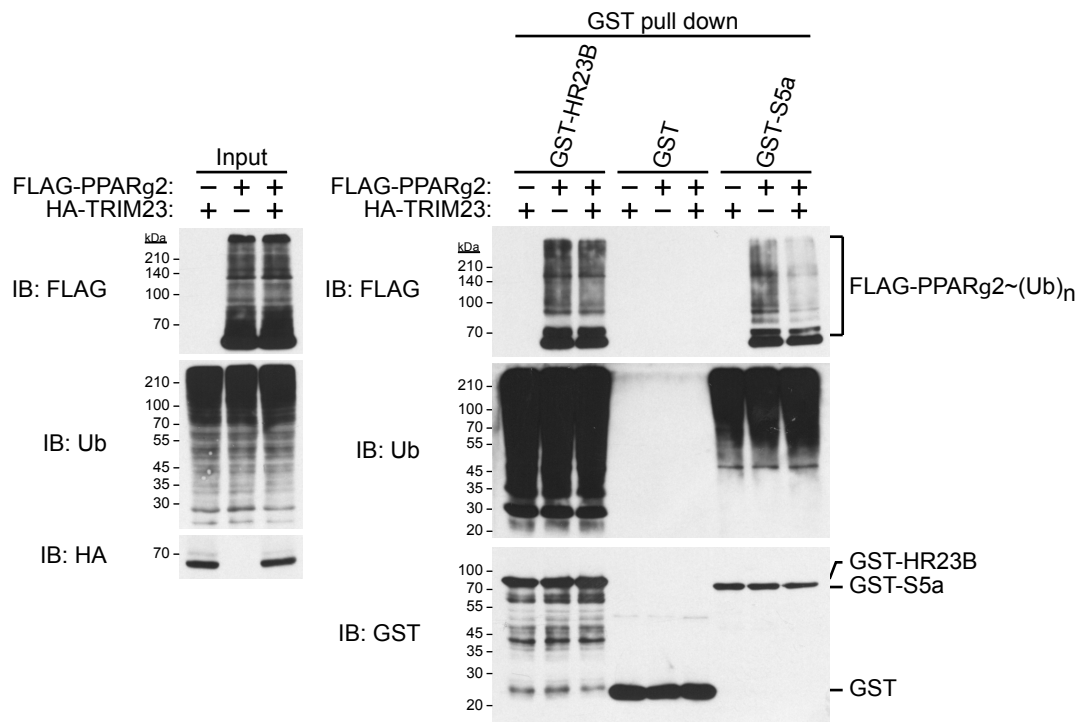




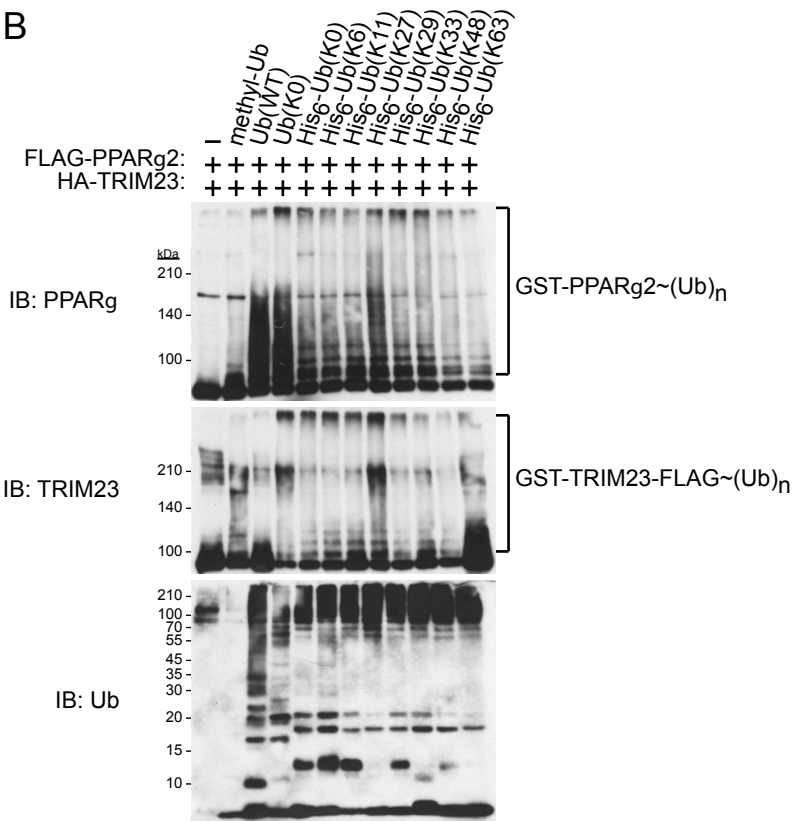
Watanabe, Figure 7



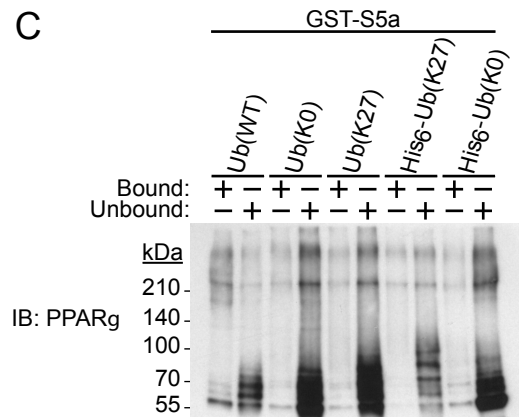
A



B



C



D

